Discover Materials

RESEARCH Open Access

Integrating recycled waste materials in cementitious grouts: evaluating mechanical integrity and rheological behaviour

Alireza Entezam[1,2*], Hadi Nourizadeh[1,2], Paulomi Polly Burey[1,4], Kevin McDougall[3], Peter Craig[5], Behshad Jodeiri Shokri[1,2], Shima Entezam[1,2], Naj Aziz[6] and Ali Mirzaghorbanali[1,2]

*Correspondence:
Alireza Entezam
Alireza.entezam@unisq.edu.au
[1]Centre for Future Materials (CFM), University of Southern Queensland, Toowoomba, QLD 4350, Australia
[2]School of Engineering, University of Southern Queensland, Springfield, QLD 4300, Australia
[3]School of Surveying and Built Environment, University of Southern Queensland, Toowoomba, QLD 4350, Australia
[4]School of Agriculture and Environmental Science, University of Southern Queensland, Toowoomba, QLD 4350, Australia
[5]Jennmar Australia Pty Ltd, Sydney, Australia
[6]School of Civil, Mining & Environmental Engineering, University of Wollongong, Wollongong, NSW 2500, Australia

Abstract

Conventional cementitious grouts, widely used for underground reinforcement and structural repair, rely heavily on Portland cement, a material responsible for nearly 7% of global CO_2 emissions and significant resource depletion. Addressing this environmental and material-efficiency challenge, this study develops and evaluates novel sustainable grout formulations that partially replace cement with recycled waste glass (WG), tyre rubber waste (TRW), and construction and demolition waste (CDW). By systematically linking mechanical, rheological, and microstructural performance, the research bridges a key gap between sustainability-driven material substitution and the performance requirements of practical grouting applications. Grout mixtures incorporating 0–20% WG, 0–3% TRW, and 0–10% CDW were evaluated for rheological behaviour and unconfined compressive strength (UCS). All modified grouts maintained shear-thinning properties but exhibited significantly reduced viscosity, enabling lower water demand. Notably, WG-enhanced grouts preserved or even improved UCS. For example, 2.5–5% WG substitution resulted in minimal strength loss, yielding up to 97% of the 70.5 MPa control strength. When adjusted for reduced water content, these mixes achieved a 10.6% UCS increase. TRW grouts peaked at 55.2 MPa with 0.75% inclusion, while CDW caused only minor strength drops at 2.5–5%. Enhanced flowability (lower viscosity/yield stress) compensated for some strength reductions. Microstructural analysis revealed that WG improved matrix density via pozzolanic activity and filler effect, while TRW and CDW influenced pore structure. Beyond their laboratory performance, these findings underscore the practical potential of recycled waste-based grouts to reduce cement consumption, lower embodied carbon, and divert waste streams from landfills. Such formulations retain pumpability and mechanical performance while offering viable alternatives for ground reinforcement, structural repair, and sustainable construction applications. Overall, the integration of WG, TRW, and CDW demonstrates a promising pathway toward lower-impact cementitious grouts that meet both engineering and environmental demands.

Keywords Cementitious grout, Waste materials, Cable bolt, Encapsulation agent, Ground support, Sustainability

1 Introduction

Cementitious grouts are formulated with varying compositions depending on the application; however, they typically consist of a blend of Portland cement, water, binders such as fly ash, and chemical additives, including superplasticisers and air detraining agents. They are used for filling cracks, connecting concrete pieces, sealing joints and reinforcing material encapsulations. The mechanical and rheological properties of grout should be tailored to suit its specific application. For example, high viscosity grouts are used for lifting structures, while fast-setting grouts are ideal for rapid sealing [52]. Grouting materials are also commonly used to enhance the strength of rock masses by injecting grout into discontinuities and cracks, thereby reinforcing the rock structure [31, 36]. In recent times, there has been a widespread utilisation of grouted rock bolts across various geotechnical, tunnelling and mining contexts, serving as both temporary and permanent ground reinforcement. A rock bolt with full grouting creates a continuous mechanically coupled (CMC) system. This system involves placing a deformed bar into a drilled hole and then filling the space around it with grout as the encapsulation agent [71]. Grout plays a critical role in the reinforcing systems as it provides the bond between the reinforcing element and the rock. This bond enables forces generated by the movement of unstable rocks to be transferred effectively from the rock mass to the reinforcing elements [17, 22].

According to [35], potential failure modes of the rock bolting system occur in the bar, at the bolt-grout interface, in the grouting material, at the grout-rock interface, and in the rock mass. In hard rock formations, the primary cause of failure typically occurs at the interface between the bolt and grout. However, in softer rock formations, the interface between the grout and rock is more susceptible [64]. While conventional Portland cement serves as the predominant binding agent in grouts due to its hardening and strengthening properties, its environmental impact necessitates the exploration of alternative solutions. Cement production is a highly energy-intensive and carbon-intensive process, contributing an estimated 7% of global greenhouse gas emissions. Therefore, developing and adopting clean and sustainable technologies in cement-based materials including grouts, is essential for addressing urban environmental challenges [32].

The incorporation of waste materials, such as tailings, fly ash, blast furnace slag, and recycled glass, into cement-based materials such as concrete and mortar presents a promising strategy for enhancing environmental sustainability [27]. This approach not only contributes to the mitigation of pressing environmental concerns like the emission of hazardous gases and various forms of pollution, but also serves as a crucial intervention in addressing the negative impacts associated with the depletion of virgin natural resources, the ever-increasing generation of solid waste streams, and the associated challenges of waste management. By promoting the utilisation of waste materials in construction applications, this practice fosters a more sustainable paradigm for the future [20, 65]. Australia generated an estimated 75.8 million tonnes of waste in 2020–21. This breakdown includes 25.2 million tonnes of building and demolition materials, 14.4 million tonnes of organics, 12.0 million tonnes of ash, 1.6 million tonnes of glass and 2.6 million tonnes of plastics [53]. Comprehensive data on all rubber waste in Australia is limited. However, the Australian Tyre Recycling Association (ATRA) reported collecting and recycling over 170,000 tonnes of end-of-life tyres annually in 2020–21. Approximately 1.5 billion tyres are anticipated to be discarded worldwide each year, and

this number is rapidly growing. Repurposing scrap tyres in construction can provide environmentally friendly solutions to tyre disposal challenges [69].

Over the past decade, the incorporation of different recycled materials has gained more attention as a partial replacement of cement in the cement and construction industries. An alternative involves using fine recycled materials from construction and demolition waste, which usually contain unhydrated cement that can produce a pozzolanic reaction [29, 58, 62]. To qualify as a standard pozzolana, a material must contain at least 70% of SiO_2, Al_2O_3, and Fe_2O_3 combined [33]. Several studies have explored the potential of waste glass for cementitious composites and have examined its use as both a partial replacement for Portland cement and as an aggregate. The high silica content of waste glass makes it a promising candidate as a precursor material in alkali-activated composites [1, 57]. Glass has a chemical composition that meets the criteria to be categorised as a pozzolan, according to previous studies [30, 51]. The literature reports that adding waste glass powder, with particle sizes of below 75 μm, at concentration of 2.5% leads to a reduction of 4.5% in compressive strength compared to the reference grout [26]. Isalam et al. [33] reported that replacing cement with up to 15% finely ground waste glass yielded 28-day compressive strengths above 40 MPa while maintaining adequate workability. Yin et al. [67] concluded that replacing cement with 15% waste glass powder improved the mini-slump flow by 12% and reduced viscosity by 20%. Additionally, both the bleeding capacity and mechanical properties were enhanced.

Lima et al. [24], explored the utilisation of construction and demolition waste (CDW) into binary and ternary cement mixtures. The fine particles (63 μm) of CDW exhibited low pozzolanic reactivity due to possessing slightly a chemical and mineralogical composition characteristic similar to that of cementitious materials. Shahidan et al. [59] investigated the effect of incorporating CDW in concrete and reported that recycled aggregate replacements reduced slump by 8–12% but retained compressive strength within 90% of control mixes. Mikos et al. [43], examined the application of recycled concrete aggregate in cementitious grout, finding that incorporation of recycled concrete cause a reduction in the flowability of the mixture.

Concrete mixtures containing rubber as aggregates exhibit low fluidity. The incorporation of rubber into the concrete results in a porous and lightweight material due to air entrapment and the hydrophobic nature of rubber [25]. These characteristics are influenced by the particle size and amount of rubber used [61]. Yuan et al., (2021) found 20–40% reductions in compressive and flexural strength at 10–20% crumb rubber addition, though toughness improved significantly. Broader aggregate research confirms that material type, replacement level, and particle size are critical. [45–47] demonstrated in a series of studies that replacing natural aggregates with Linz–Donawitz slag can preserve compressive and tensile strength within 5–10% of conventional mixes when dosage remains below 30%.

The rheological characteristics of grouts, including plastic viscosity, yield stress, and thixotropy, must be optimised to meet the specific requirements of the application. These properties are essential as they directly influence the material's workability, pumpability, self-leveling capability, compaction, and initial setting time in practical engineering applications [16, 38]. The required pump pressure for conveying grouts through pipelines and injecting them into boreholes also depends on the frictional characteristics and the particle size of the ingredients [3]. [54] demonstrated that the rheological

properties of cementitious grouts are quite complex due to their unpredictable yield stress and thixotropy. [67] concluded that incorporating waste glass powder, superplasticiser, and viscosity modifying agents into cement-based grouting materials adhered to the Herschel-Bulkley rheological model and displayed a notable shear thickening behaviour. [40] conducted a series of experiments to examine the influence of different components on the rheological behaviour of cementitious grouts. For Clay-Cement Slurry, the rheological characteristics are determined by the water-to-solid ratio and the amount of clay used. In contrast, for Clay-Cement Pasty Slurry, the rheological behaviour is primarily affected by the amount of modifier added, shifting from rheopexy to thixotropy as the modifier dosage increases.

Unlike earlier studies such as [19], which primarily examined sand additions to enhance grout stiffness and pull-out strength in rock anchors, several critical knowledge gaps remain. First, most investigations of recycled waste materials have been conducted in concrete or mortars rather than in cementitious grouts, which have unique requirements for pumpability, borehole encapsulation, and long-term bond integrity in underground conditions. Second, there is limited integration of rheological and mechanical performance in the same experimental framework, even though both properties govern in situ behaviour. Third, the effect of waste inclusion on load transfer mechanisms in fully grouted reinforcement systems remains largely unexplored, with existing research focusing primarily on bulk strength rather than bond efficiency.

This study addresses these gaps by systematically evaluating cementitious grouts modified with finely ground waste glass (WG), tyre rubber waste (TRW), and CDW. The novelty lies in bridging sustainability-driven material substitution with performance-critical grout functions, combining mechanical, rheological, and microstructural assessments within one program. The objectives are to (i) quantify the effects of WG, TRW, and CDW on compressive strength and elastic modulus; (ii) evaluate rheological performance relevant to pumpability and borehole encapsulation; and (iii) interpret microstructural modifications in relation to bond and load transfer. By aligning environmental imperatives with engineering reliability, this research establishes a framework for developing sustainable grout formulations tailored to mining and tunnelling reinforcement.

2 Materials and methods

The choice of waste materials for incorporation into cementitious grout depends on several factors, including desired properties of the grout, cost and availability of waste materials, compatibility with the grout mix and environmental considerations. Recycled WG, TRW, and CDW in the form of crusher dust were chosen for several reasons as each brings distinct contributions to the grout formula apart from cost-effectiveness and sustainability including:

- WG may contribute to the pozzolanic reaction, enhancing the strength and durability of the grout.
- The elasticity and flexibility of TRW particles may enhance the ductility and shear modulus of the grout and consequently may enhance the distribution of the bond stress along the encapsulation length.
- CDW is an ideal replacement for grout containing trace amounts of cement, reducing the demand for natural resources. Additionally, the literature indicates that

incorporating fine aggregates can enhance the bearing capacity of the reinforcing system.

The waste materials were incorporated as partial replacements of the binder component after the initial mixing stage. WG was introduced in four particle-size ranges, < 75 µm, 75–150 µm, 150–300 µm, and 300–425 µm, and at five replacement levels of 2.5%, 5%, 10%, 15%, and 20% by weight of grout, resulting in twenty distinct WG mixtures. CDW was tested in two particle-size ranges, 150–300 µm and 300–600 µm, at replacement levels of 2.5%, 5%, 7.5%, and 10%. TRW was evaluated in two size ranges, < 300 µm and 300–600 µm, with replacement levels of 0.75%, 1.5%, 2.25%, and 3%. The maximum WG replacement level of 20% was selected based on preliminary investigations by [26] while TRW and CDW dosages were adjusted volumetrically to achieve equivalence with the corresponding WG proportions.

The bulk densities of the raw materials were determined prior to mixing to ensure accurate proportioning and volume consistency among the grout mixtures. The measured bulk densities were 1214 kg/m^3 for WG, 337 kg/m^3 for TRW, 986 kg/m^3 for CDW, and 883 kg/m^3 for the grout matrix. These differences reflect the varying particle morphology and porosity of each material; TRW exhibiting the lowest density due to its elastic, cellular structure, and WG the highest as a result of its compact nature. The density contrast among materials was considered when calculating volumetric replacement ratios to maintain equivalent solid volumes across all grout formulations.

Particle size distribution of the waste materials was determined through standard sieve analysis in accordance with ASTM C136/C136M-19 [11] and the equivalent Australian code AS 1141.11.1:2020 Amd 1 [5] following recommended practices outlined in recent studies [50]. The results are presented in Fig. 1. The median particle size for WG and TRW was 320 µm, and their particle size distributions were closely comparable, with the two curves nearly overlapping. In contrast, CDW exhibited a larger median particle size of 1.4 mm.

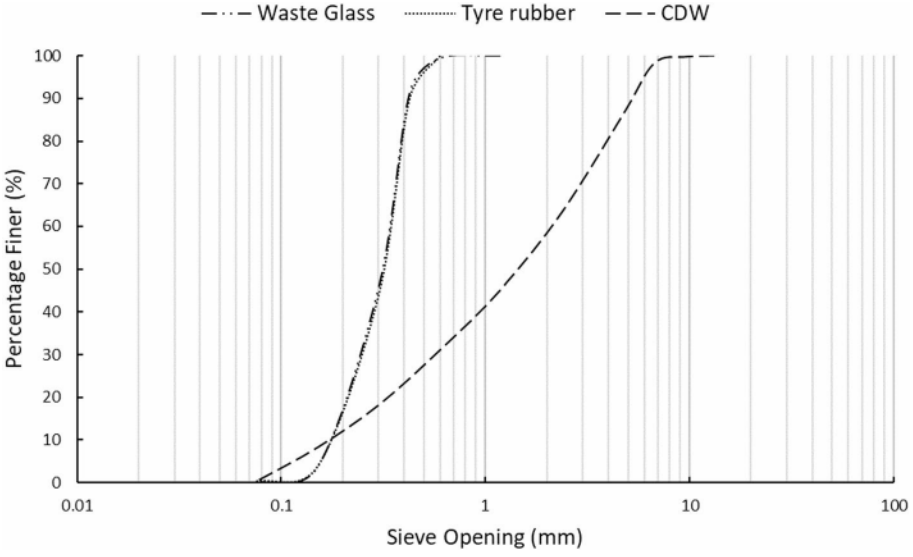

Fig. 1 Particle size distribution of the waste materials. WG and TRW exhibit nearly identical PSDs (median ≈ 320 µm) due to similar processing fineness

Scanning electron microscope (SEM) analysis was performed on the raw materials using a JCM6000 benchtop microscope to observe the morphology of the materials, complementing traditional sieve analysis. The SEM analysis, shown in Fig. 2, revealed that WG particles have sharp edges, while TRW particles show smooth, irregular surfaces, and CDW particles display a mix of angular and rounded shapes while the grout demonstrated a flaky pattern with fine particles.

To visually summarise the experimental methodology, a schematic flowchart is provided in Fig. 3, outlining the key phases of the study from material selection to testing. This includes particle characterisation, grout formulation, sample casting, and the full suite of mechanical and rheological evaluations. The flowchart also highlights the interconnection between various characterisation techniques and iterative feedback for formula optimisation, ensuring both performance benchmarking and reproducibility.

3 Testing design

A comprehensive testing regime was implemented to evaluate the impact of recycled waste materials on cementitious grouts. This included investigations into compressive strength, elastic modulus, microstructural properties, and rheological characteristics. Samples were mixed and prepared with various water-to-grout ratios (W/G) and it was found that W/G ratio of 40% was the most suitable considering consistent flowability, pumpability, initial setting time and minimum shrinkage. The mix design of grouts were summarised in Table 1. Consistent mixing procedures were employed for all mixtures to ensure the reliability and consistency of the results.

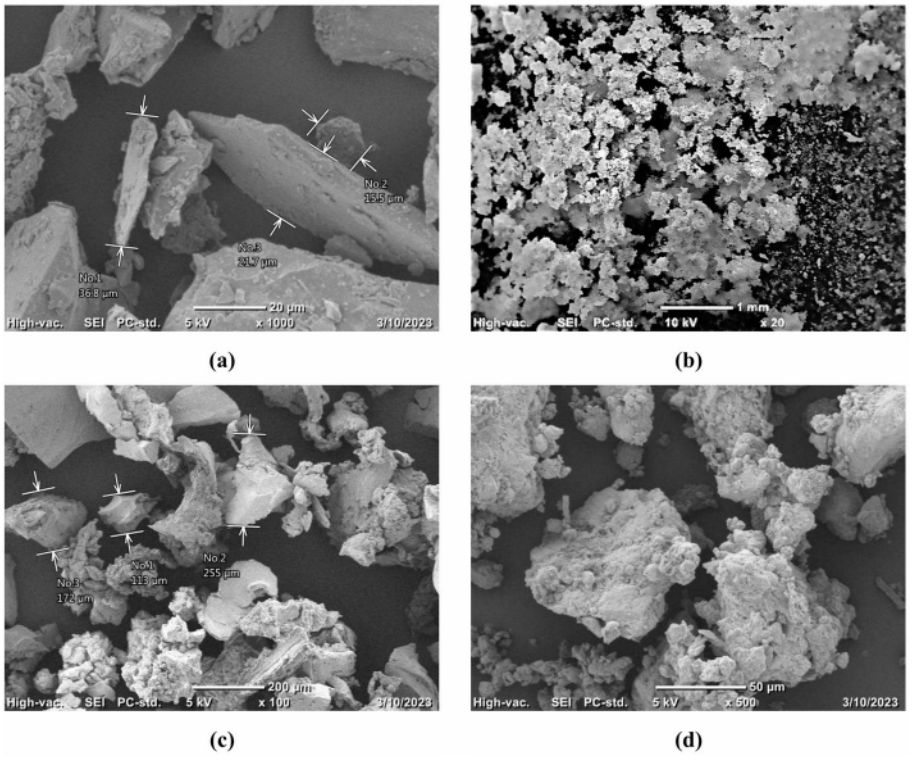

Fig. 2 SEM images on the raw materials (**a**) WG powder below 75 µm (**b**) plain grout particles (**c**) TRW 150–300 µm (**d**) CDW 75–150 µm

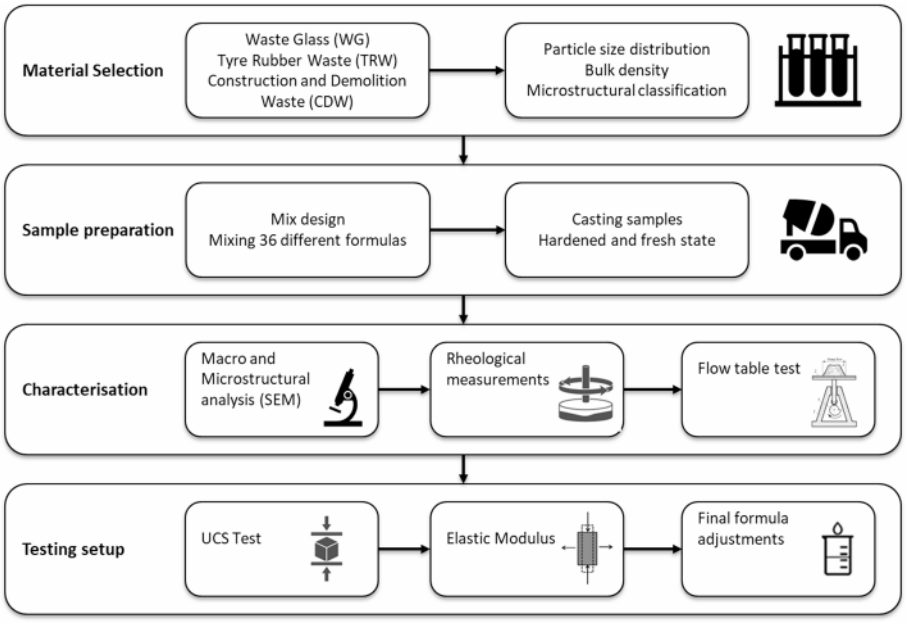

Fig. 3 Schematic overview of the experimental program, including material selection, sample preparation, testing setup, and characterisation techniques

3.1 Mechanical characteristics

An extensive experimental campaign was conducted to measure the unconfined compressive strength (UCS) of the developed amended grouts. The mixtures were prepared using a 5 L industrial planetary mixer following ASTM C305-20 [13] and AS 1012.9 [4] procedures, maintaining a constant mixing speed and sequence for all batches. The mixing duration was standardised at 30 ± 2 s for dry blending and 90 ± 5 s after water addition to ensure complete dispersion of cement and waste particles. Throughout the process, ambient temperature was maintained at 20 °C. After casting, the 50 × 50 × 50 mm cubic specimens were demoulded after 24 h and transferred to a curing chamber set to 20 °C and relative humidity of 90%, in accordance with ASTM C109/C109M-24 [9]. These parameters mirror common curing conditions used in industry-scale grout preparation and are consistent with established concrete testing practice [48]. The UCS of grout cubes was determined in accordance with the domestic standard AS 1012.9 [4] which is equivalent to ASTM C109/C109M-24 [9]. The procedure follows recent practice in sustainable grout and concrete research [44, 47]. The tests were carried out on all the mixtures listed in Table 1, for curing periods of 7, 14, 21, and 28 days, using Impact 2000 kN MTS machine with a 300 kN load-cell connected to the data acquisition system. A total of 720 samples were cast and tested. Twenty additional samples of the plain grout without any waste materials were tested as the control samples. Each test was repeated five times to ensure consistency with any erroneous samples omitted and then the average value was reported.

Elastic modulus (E) of the samples also was quantified for each mixture. Elastic modulus is crucial as it affects the bonding behaviour, axial load transfer mechanism of fully grouted bolting systems specifically at the bolt-grout interface [68, 70].

By aligning all procedures with standardised methods and maintaining identical environmental and mix parameters across the entire experimental matrix, potential variability due to operator influence or ambient fluctuation was minimised. This approach

Table 1 Mix design of the cementitious Grout materials

Mix No.	WG (%)	TRW (%)	CDW (%)	Particle size range (μm)	W/G (%)
1	0	0	0	-	40
2	2.5	0	0	< 75	40
3	2.5	0	0	75–150	40
4	2.5	0	0	150–300	40
5	2.5	0	0	300–425	40
6	5	0	0	< 75	40
7	5	0	0	75–150	40
8	5	0	0	150–300	40
9	5	0	0	300–425	40
10	10	0	0	< 75	40
11	10	0	0	75–150	40
12	10	0	0	150–300	40
13	10	0	0	300–425	40
14	15	0	0	< 75	40
15	15	0	0	75–150	40
16	15	0	0	150–300	40
17	15	0	0	300–425	40
18	20	0	0	< 75	40
19	20	0	0	75–150	40
20	20	0	0	150–300	40
21	20	0	0	300–425	40
22	0	0.75	0	< 300	40
23	0	0.75	0	300–600	40
24	0	1.5	0	< 300	40
25	0	1.5	0	300–600	40
26	0	2.25	0	< 300	40
27	0	2.25	0	300–600	40
28	0	3	0	< 300	40
29	0	3	0	300–600	40
30	0	0	2.5	150–300	40
31	0	0	2.5	300–600	40
32	0	0	5	150–300	40
33	0	0	5	300–600	40
34	0	0	7.5	150–300	40
35	0	0	7.5	300–600	40
36	0	0	10	150–300	40
37	0	0	10	300–600	40

enhances the reproducibility of the results and facilitates comparison with other experimental and industrial studies on cementitious grouts.

3.2 Microstructural studies

Microstructural studies were conducted using SEM model JEOL JMC-6000 to understand the internal structure of the amended grout matrix, focusing on the distribution of hydration products, porosity, and bonding phases, in comparison to the plain grout. More importantly, these studies analysed the distribution of waste materials within the matrix and the bonding interactions between the waste materials and the matrix (Dobiszewska et al. (2023). SEM observations followed the guidelines of ASTM C1723-25 [14]. These procedures are consistent with state-of-the-art studies evaluating recycled binders in cementitious composites [46, 47].

Elemental composition analysis was performed using an iXRF ATLAS X X-ray fluorescence/mapping (XRF/XFM) system operated in vacuum mode following the procedures of ASTM C114-24 [10] and AS 2350.2 [6], to determine oxide distribution and compositional variation in grout specimens incorporating WG.

3.3 Rheological assessments

An understanding of viscosity dependence on shear rate is crucial for understanding the effects of the incorporation of waste materials on the workability and pumpability of the grouts. By analysing this rheological behaviour, the grout formulations can be optimised to achieve desired performance characteristics for specific applications, such as cable bolting systems. All grout samples were homogenised using a planetary mechanical stirrer and shear rate sweeps were carried out on all samples using an Anton Paar MCR502 equipped with a PP50 D parallel-plate geometry and a Peltier-based temperature control system as illustrated in Fig. 4. The test temperature was maintained at 25 °C throughout the procedure to eliminate temperature-induced variations in viscosity. The rheological test began at 1 mm sample size gap with a 60-second hold after sample loading. Subsequently, the sample was subjected to a pre-shear at a rate of 0.01 s^{-1}. The shear rate sweep was then undertaken across a range of 0.01–100 s^{-1}. While no specific Australian Standard currently exists for grout rheology, the procedure was guided by ASTM C1749-25 [15]. The approach follows recent international studies on the rheology of cementitious grouts and sustainable binders [44], [55].

3.4 Flowability and consistency measurements

The flowability of grout mixes was evaluated using the flow table method in accordance with AS 2701-2001 (R2015) [7]. This procedure is equivalent to ASTM C230/C230M-23 [12]. Flow values were recorded as the average spread diameter after the prescribed number of drops. The test method has been widely applied for assessing the fresh-state

Fig. 4 (**a**) The Anton Paar MCR502 automatic rheometer (**b**) PP50 D

performance of cementitious grouts and mortars, particularly in the development of sustainable formulations with recycled materials [44], [55].

4 Results and discussion

4.1 Compressive strength

The compressive strength of the cementitious grouts varied substantially with the type, particle size, and replacement percentage of recycled waste materials. As illustrated in Fig. 5, mixes incorporating finely ground waste glass (WG) exhibited the most promising results, particularly at lower replacement levels (2.5–5%). The UCS of these samples reached up to 97% of the control strength (70.5 MPa at 28 days) and in some cases exceeded the reference when water content was optimised. Section 4.8 delves into this topic in more detail.

The underlying mechanism for this performance is attributed to the pozzolanic activity and filler effect of WG. The amorphous silica in WG reacts with calcium hydroxide during hydration, producing additional calcium silicate hydrate (C–S–H) gel, which densifies the microstructure and enhances long-term strength [2]. This effect is particularly evident in finer particles (< 75 µm), which offer a higher surface area for reaction. In contrast, higher WG contents (15–20%) led to strength reductions due to dilution of cementitious phases and increased porosity.

In contrast, the incorporation of tyre rubber waste (TRW) resulted in a more pronounced decline in UCS (Fig. 6). This behaviour stems from the low stiffness, hydrophobicity, and poor bonding characteristics of rubber particles. These properties prevent the formation of strong interfacial zones, induce entrapped air, and lead to void formation, as observed in macro and SEM images (Figs. 12 and 14 a, b). Despite these drawbacks, TRW may contribute positively to ductility and toughness, albeit at the expense of compressive performance.

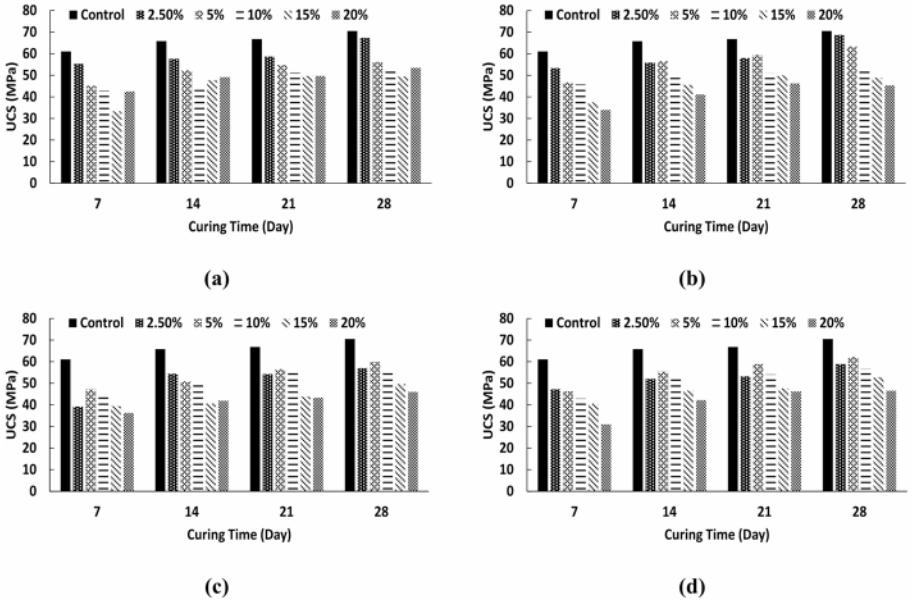

Fig. 5 Compressive strength of samples with 0–20% WG content within particle size range of (**a**) < 75 µm (**b**) 75–150 µm (**c**) 150–300 µm (**d**) 300–425, over time

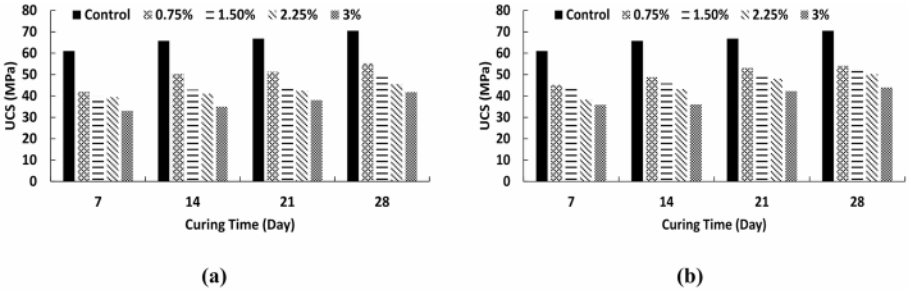

Fig. 6 Compressive strength of samples with 0-3% TRW content within particle size range of (**a**) <300μm (**b**) 300-600μm, over time

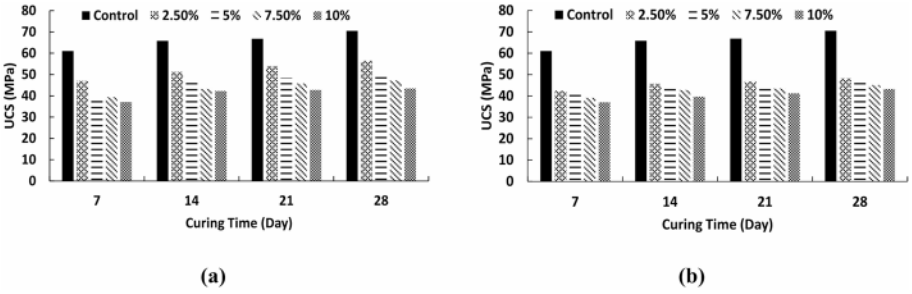

Fig. 7 Compressive strength of samples with 0-10% CDW content within particle size range of (**a**) 150-300 μm (**b**) 300-600 μm, over time

While TRW particle size did not exhibit a consistent influence on strength, it is possible that finer particles may have a greater impact on the interfacial transition zone between the rubber and cement phases. This zone is critical for load transfer and crack resistance, and its properties can be significantly affected by particle size and shape [69].

For construction and demolition waste (CDW), UCS values also declined with increasing content, though the rate of reduction was moderate at lower dosages (2.5–5%) (Fig. 7). CDW acts mainly as an inert filler, contributing little to hydration [24]. SEM images (Fig. 14 c, d) revealed sparse C–S–H formation and persistent pore structures. However, the presence of residual unhydrated cement particles and fines may marginally contribute to later-age strength through limited pozzolanic effects.

These findings suggest that WG is the most effective additive for preserving strength, provided its content and particle size are carefully optimised. TRW and CDW reduce strength more significantly, primarily due to interfacial weaknesses and binder dilution, respectively.

Although several waste-modified mixes showed statistically significant reductions in UCS relative to the control, these differences are not necessarily critical when evaluated against design benchmarks for grouting applications in mining and tunnelling. Industry practice typically requires grout materials used for rock bolt or cable bolt encapsulation to achieve a 28-day UCS above 25–40 MPa for temporary supports and 50 MPa for permanent installations [22, 23]. In this study, even the weakest formulations—those containing up to 20% WG, 3% TRW, or 10% CDW, maintaind UCS vlues exceedig 40 MPa, with most WG-modified grouts achieving between 53 and 67 MPa. These results confirm that all tested grouts satisfy, and in many cases surpass, the minimum strength criteria for encapsulation materials used in ground-support systems.

Furthermore, in practical applications, bond efficiency and shear transfer along the grout–rock–bolt interface govern overall reinforcement performance more than the bulk compressive strength of the grout itself [68, 71]. Hence, modest UCS reductions, particularly when accompanied by improved flowability, lower viscosity, and more complete encapsulation, can still yield superior in-situ performance. The observed behaviour of the waste-modified mixes, especially those with low-dosage waste glass, therefore represents a balanced and structurally acceptable trade-off between sustainability, workability, and mechanical reliability for mining-related grouting applications.

4.2 Statistical validation of unconfined compressive strength (UCS) results

To statistically validate the observed differences in 28-day UCS across grout formulations, a two-tailed independent t-test was conducted for each modified mix against the control. The analysis was based on five specimens per group, and a significance level of $\alpha = 0.05$ was used. Table 2 summarises the mean UCS, standard deviation (SD), p-value, and statistical significance for each mixture.

The control mix achieved a 28-day UCS of 70.5 ± 1.44 MPa. Among the modified mixes, only the sample with 2.5% waste glass (WG) of < 0.75 µm particle size had a mean UCS (67.3 MPa) that was not statistically different from the control ($p = 0.069$). All other WG mixtures, particularly at higher replacement levels (≥ 5%), demonstrated statistically significant reductions in strength ($p < 0.001$). The UCS declined progressively with increasing WG content, reaching 44.4 MPa at 20% WG ($p < 0.00001$), reflecting dilution of the cementitious phase and lower matrix integrity.

Mixtures containing tyre rubber waste (TRW) showed substantial strength loss even at low replacement levels. For example, 0.75% TRW (< 300 µm) yielded a UCS of 52.1 ± 1.59 MPa ($p < 0.0001$), which was significantly lower than the control. This trend intensified with increasing TRW content, confirming that the elasticity and hydrophobicity of rubber severely disrupt the cement matrix.

In the case of construction and demolition waste (CDW), even 2.5% CDW (150–300 µm) resulted in a significant UCS reduction to 56.5 MPa ($p = 0.0008$). Higher CDW dosages further lowered strength, with UCS dropping below 50 MPa in several formulations. These results are consistent with the low reactivity and pore-generating characteristics of CDW fines.

Collectively, the statistical analysis confirms that all mixes except one (WG < 0.75 µm, 2.5%) exhibited 28-day UCS values that were significantly different from the control ($p < 0.05$). This reinforces the earlier trend-based observations and demonstrates the importance of both dosage and particle size when incorporating recycled materials in grout design.

4.3 Elastic modulus: correlation with strength and structural mechanisms

Elastic modulus (E) results at 28 days, shown in Fig. 8 , closely followed the trends observed in compressive strength (Figs. 5, 6, 7), reinforcing the mechanical relationship between stiffness and UCS. All waste-modified grouts exhibited reductions in E compared to the reference grout (7.0 GPa), with the degree of reduction depending on both the type and proportion of waste material.

Mixes incorporating 2.5–5% WG, especially with < 75 µm particle size, retained E values above 6.6 GPa, an indication of their dense microstructure and refined pore

Table 2 Statistical analysis of 28-day UCS for modified Grouts vs. control

Mix ID	Mean UCS (MPa)	SD	*p*-value vs. Control	$p < 0.05$ (Significant)
Control (0% waste)	70.5	1.44	–	–
2.5% WG (< 75 µm)	67.3	1.71	0.069288783	No
5% WG (< 75 µm)	56.2	0.78	0.000111159	Yes
10% WG (< 75 µm)	52.4	0.38	3.02492E-05	Yes
15% WG (< 75 µm)	49.4	1.73	8.48518E-05	Yes
20% WG (< 75 µm)	53.5	1.34	0.000115572	Yes
2.5% WG (75–150 µm)	68.7	3	0.405315928	No
5% WG (75–150 µm)	63.4	1.56	0.004409763	Yes
10% WG (75–150 µm)	53.5	2.7	0.000646737	Yes
15% WG (75–150 µm)	48.9	0.4	1.51855E-05	Yes
20% WG (75–150 µm)	45.4	1.17	1.99011E-05	Yes
2.5% WG (150–300 µm)	57	2.9	0.002034826	Yes
5% WG (150–300 µm)	59.9	2.89	0.004655024	Yes
10% WG (150–300 µm)	55.6	2.26	0.00064496	Yes
15% WG (150–300 µm)	49.6	1.29	4.84932E-05	Yes
20% WG (150–300 µm)	46	1	1.73692E-05	Yes
2.5% WG (300–425 µm)	58.9	1.46	0.000601763	Yes
5% WG (300–425 µm)	62.2	0.57	0.000751897	Yes
10% WG (300–425 µm)	56.8	0.36	8.99816E-05	Yes
15% WG (300–425 µm)	52.9	1	6.45433E-05	Yes
20% WG (300–425 µm)	46.5	0.59	1.18806E-05	Yes
0.75% TRW (< 300 µm)	55.25	2.21	0.000110453	Yes
1.5% TRW (< 300 µm)	49.48	0.87	0.000159562	Yes
2.25% TRW (< 300 µm)	45.55	1.9	6.47194E-06	Yes
3% TRW (< 300 µm)	41.78	1.14	1.56405E-05	Yes
0.75% TRW (300–600 µm)	54.13	1.57	4.88051E-05	Yes
1.5% TRW (300–600 µm)	52.51	0.82	0.000314839	Yes
2.25% TRW (300–600 µm)	50.24	1.08	7.14619E-05	Yes
3% TRW (300–600 µm)	43.95	0.59	0.000282837	Yes
2.5% CDW (150–300 µm)	56.5	0.5	0.001758839	Yes
5% CDW (150–300 µm)	50.75	0.64	0.000490169	Yes
7.5% CDW (150–300 µm)	47.2	0.67	0.000285039	Yes
10% CDW (150–300 µm)	43.5	0.4	0.00051811	Yes
2.5% CDW (300–600 µm)	48.2	0.55	0.000502513	Yes
5% CDW (300–600 µm)	46.9	0.53	0.000474215	Yes
7.5% CDW (300–600 µm)	45.1	0.69	0.000204014	Yes
10% CDW (300–600 µm)	43.3	0.64	0.000211349	Yes

network, supported by SEM observations (Fig. 11 a, b). This is a direct consequence of the pozzolanic reactivity of WG, which enhances secondary C–S–H formation and reduces porosity [18]. As the WG content increased beyond 10%, the modulus declined due to a reduced cement phase and the formation of weaker interfacial zones.

In the case of TRW, elastic modulus suffered the most significant reduction (Fig. 8 b), in some cases dropping by over 40%. The main cause is TRW's soft, elastic nature and incompatibility with the cement matrix, which leads to poor stress transfer and the formation of voids and discontinuities at the interface [61]. This was confirmed through macroscopic imaging and SEM analyses (Figs. 12 and 14 a, b), which showed dispersed rubber particles and entrapped air pockets.

The CDW-modified grouts exhibited moderate reductions in modulus (Fig. 8 c), primarily due to dilution of the cementitious binder and the limited chemical reactivity of

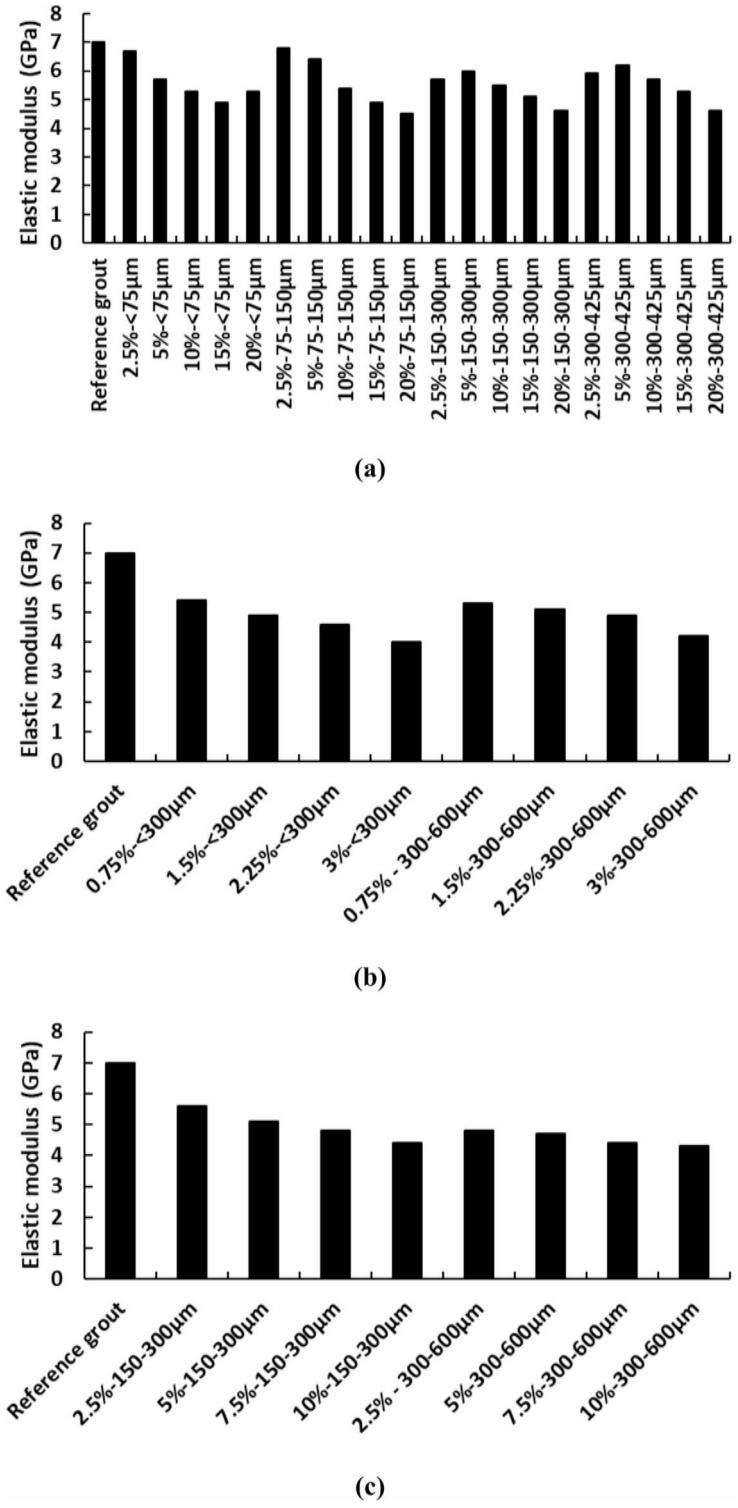

Fig. 8 Elastic modulus of the samples at 28 days of curing incorporating (**a**) WG (**b**) TRW (**c**) CDW

CDW particles. SEM images (Fig. 14 c, d) demonstrated weaker bonding networks and a less uniform C–S–H matrix.

The correlation between UCS and elastic modulus across all mixes was statistically robust, with R^2 values exceeding 0.95 (Fig. 9). This confirms that strength development

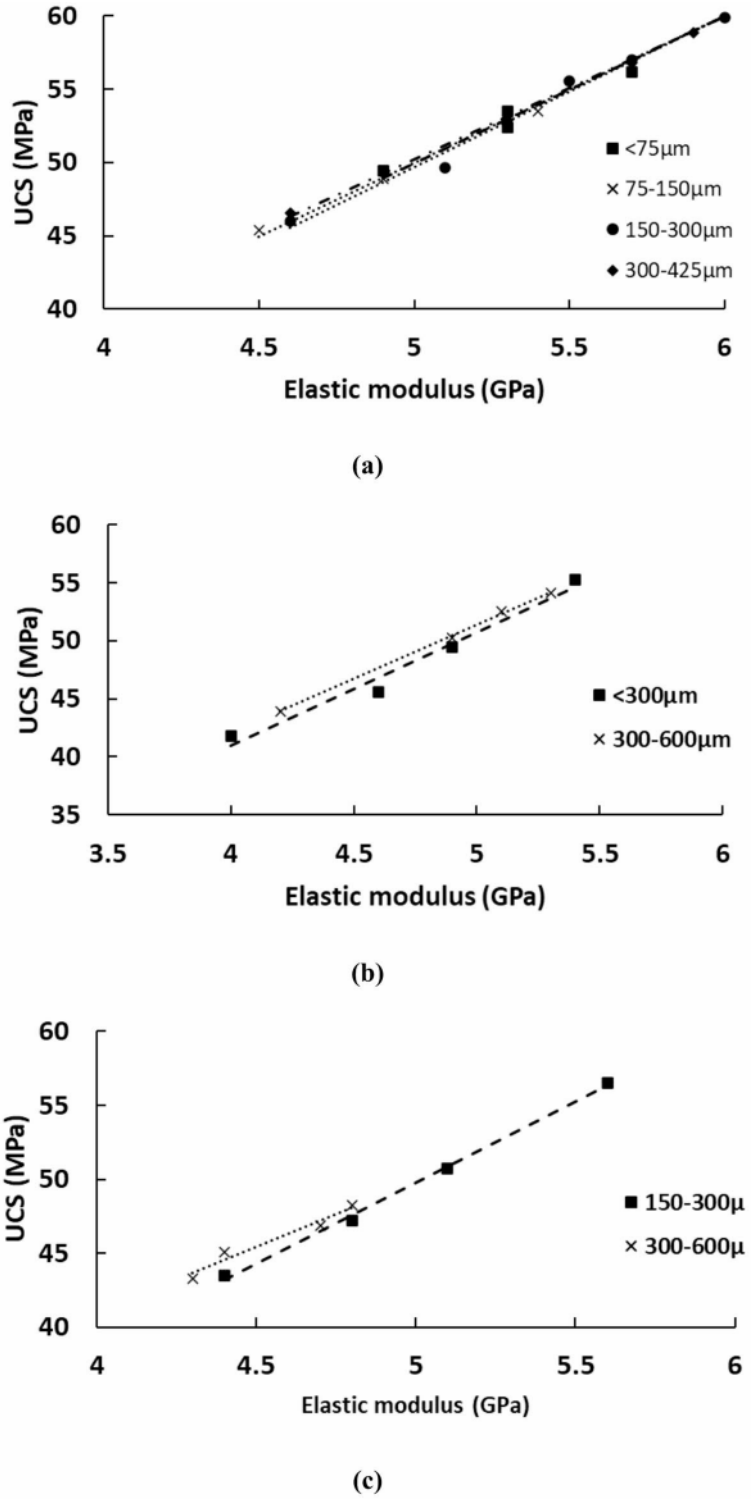

Fig. 9 The relationship between UCS and elastic modulus incorporating (**a**) WG, R^2 range 0.98-0.99 (**b**) TRW, R^2 range 0.97-0.99 (**c**) CDW, R^2 range 0.95-0.99

and stiffness are both governed by the internal structure, interfacial bonding, and hydration efficiency influenced by the incorporated waste materials.

To further interpret the mechanical behaviour of the waste-modified grouts, separate regression analyses were performed for the UCS–E relationships of the WG, TRW, and CDW series. All three categories exhibited strong linear correlations ($R^2 \geq 0.92$), consistent with the proportional relationship between compressive strength and stiffness reported for cementitious materials [17, 23]. However, the regression slopes differed noticeably among the waste types. WG mixes showed the steepest slope, reflecting enhanced stiffness development through pozzolanic densification and improved particle packing. TRW mixes exhibited the lowest slope due to the compliant and elastic nature of rubber particles, which reduce load-transfer efficiency within the matrix, while CDW mixtures displayed intermediate behaviour, likely influenced by partial reactivity of residual unhydrated cement and fine filler effects.

A one-way ANCOVA confirmed that these slope differences were statistically significant ($p < 0.05$), indicating that each recycled material type follows a distinct stiffness–strength scaling mechanism. Such differentiation has practical relevance for grout design, since stiffness governs confinement efficiency, crack bridging, and bond transfer in fully grouted reinforcement systems [68, 71].

4.4 Macro-micro analysis

Macro and micro investigation, depicted in Figs. 10 and 11 respectively. Figure 10 presents macromorphological images (6x magnification) of grout samples incorporating WG powder. A uniform distribution of WG particles is evident throughout the samples, with no discernible segregation compared to the plain grout (Fig. 10 a). Glass particles are visible on a macro scale, as highlighted in Fig. 10 h and d Additionally, the formation of pores, as illustrated in Fig. 10 b and d, may contribute to the nucleation and propagation of cracks, potentially compromising the ultimate strength of the samples.

SEM analysis was conducted to examine the morphology of the grout incorporating waste glass. Prior to testing, all samples were coated with a thin layer of gold. Figure 11 illustrates a compact structure characterized by the presence of calcium silicate hydrate (C–S–H) gel and calcium hydroxide (C–H) in the form of large hexagonal crystalline plates. The phase identification presented in Fig. 11 is based on the distinctive morphology of the hydration products: hexagonal plate-like crystals consistent with $Ca(OH)_2$ (portlandite) and adjacent fibrous regions corresponding to C–S–H gel. Although EDS analysis was not performed, the XRF/XFM results support this interpretation by showing reduced Ca and increased Si concentrations in WG-modified grouts, consistent with the progressive formation of C–S–H. These features align with hydration microstructures reported in previous studies [1, 51]. The inclusion of WG powder serves as a filler within the matrix. The grout components and glass particles are encapsulated within a dense, C–S–H gel-rich network, enhancing the material's compressive strength. Partial replacement of grout with WG powder resulted in a reduction of C–H crystals and the formation of a denser, more uniform structure (Fig. 11 a, b). This improvement is attributed to the pozzolanic reaction of WGP, where C–H is transformed into C–S–H gel, as well as the filler effect, with fine WGP particles filling the micro-pores in the matrix [18]. However, samples containing 2.5–5% WGP exhibited a more compact structure

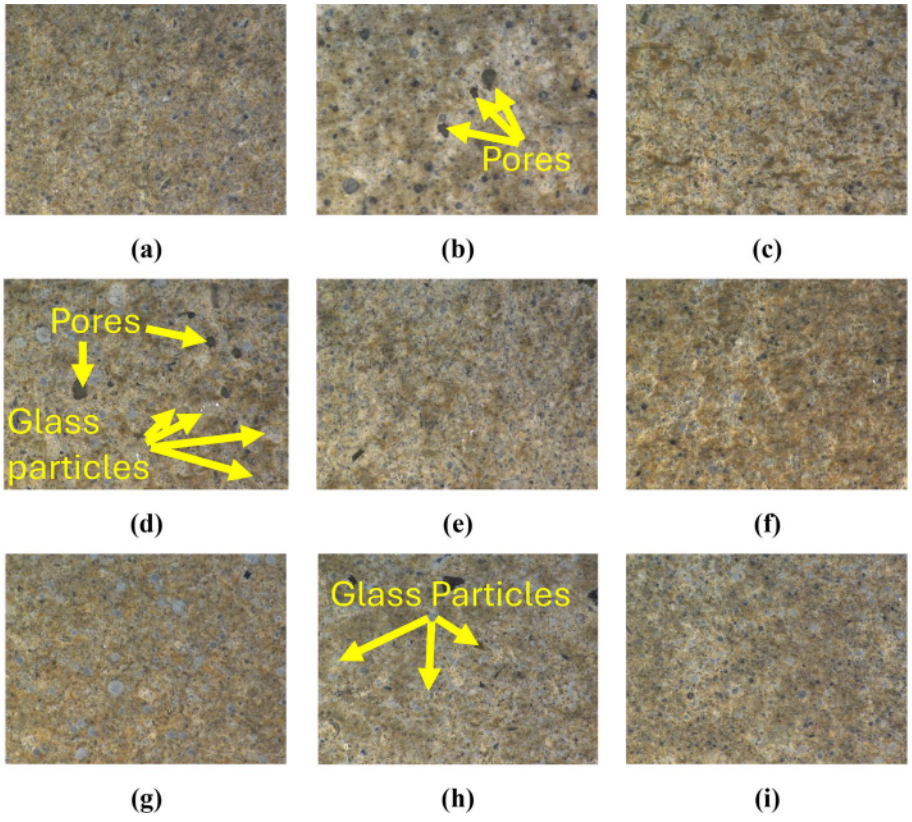

Fig. 10 Macro imaging of the samples using WG captured at 6x magnification including (a) Control grout (b) 20% glass <75 µm (c) 20% glass 75-150 µm (d) 20% glass 150-300 µm (e) 20% glass 300-425 µm (f) 5% glass <75 µm (g) 5% glass 75-150 µm (h) 5% glass 150-300 µm (i) 5% Glass 300-600 µm

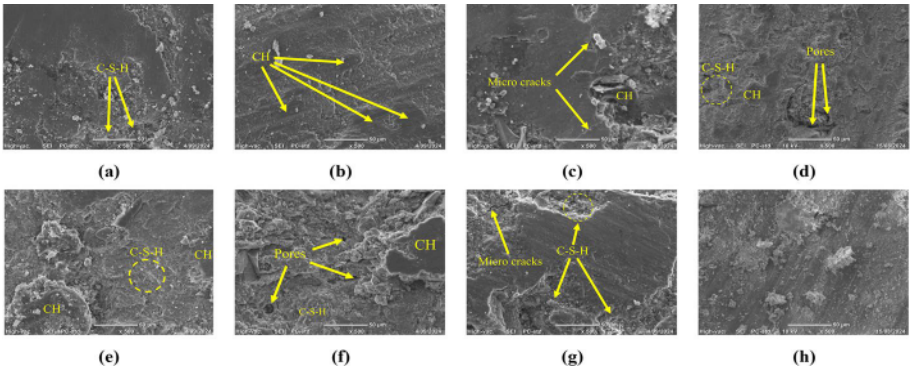

Fig. 11 Micromorphology of the grout samples with WG including (**a**) 2.5% glass 300-425 µm (**b**) 5% glass 75-150 µm (**c**) 10% glass <75 µm (**d**) 10% glass 150-300 µm (**e**) 10% glass 300-425 µm (**f**) 20% glass <75 µm (**g**) 20% glass 150-300 µm (**h**) 20% glass 300-425 µm

compared to those with 20% WGP (Fig. 11 f, g, h). This is because higher replacement levels reduce the grout content, leading to less binder production.

Figure 12 depicts grouts containing TRW at varying percentages and particle sizes, showcasing a heterogeneous surface with prominent air pockets and voids. The irregular distribution of components and surface imperfections are clearly visible, indicating a lack of uniformity within the matrix. In contrast, Fig. 13 illustrates grouts incorporating CDW at different particle sizes and percentages, exhibiting a more uniform surface

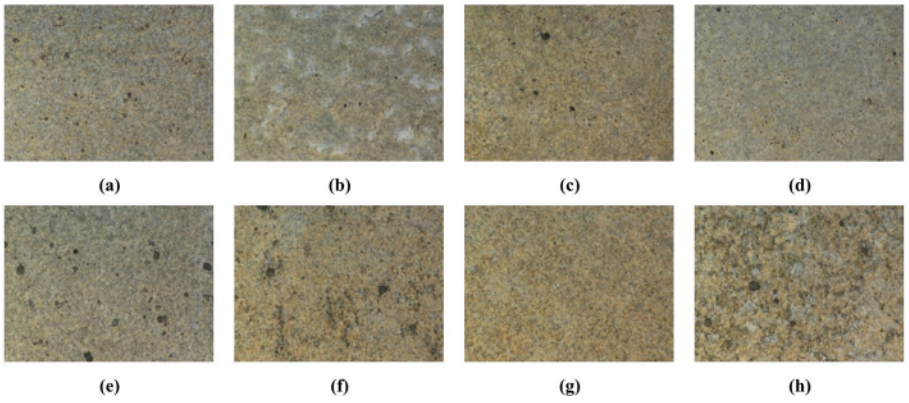

Fig. 12 Macro imaging of the grout samples with TRW captured at 6x magnification including (**a**) 0.75% TRW <300 µm (**b**) 1.5% TRW <300 µm (**c**) 2.25% TRW <300 µm (**d**) 3% TRW <300 µm (**e**) 0.75% TRW 300-600 µm (**f**) 1.5% TRW 300-600 µm (**g**) 2.25% TRW 300-600 µm (**h**) 3% TRW 300-600 µm

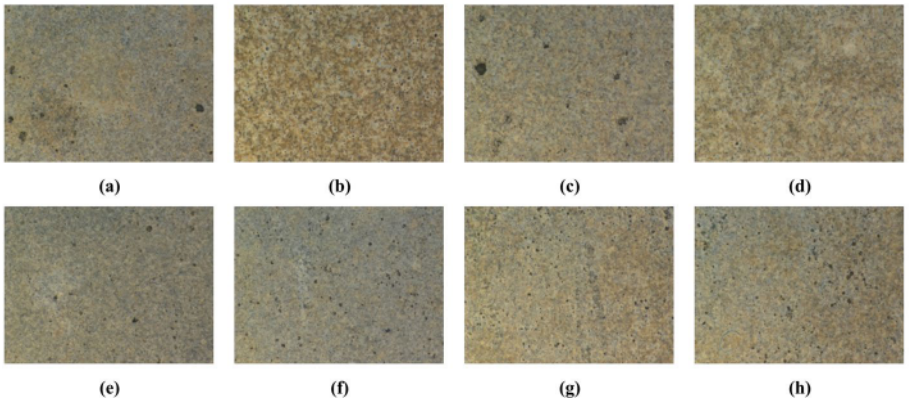

Fig. 13 Macro imaging of the grout samples with CDW captured at 6x magnification including (**a**) 2.5% CDW 150-300 µm (**b**) 5% CDW 150-300 µm (**c**) 7.5% CDW 150-300 µm (**d**) 10% CDW 150-300 µm (**e**) 2.5% CDW 300-600 µm (**f**) 5% CDW 300-600 µm (**g**) 7.5% CDW 300-600 µm (**h**) 10% CDW 300-600 µm

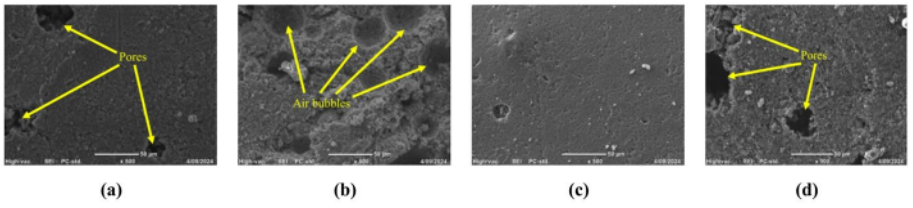

Fig. 14 Micromorphology of the grout samples with TRW and CDW including (**a**) 3% TRW <300 µm (**b**) 3% TRW 300-600 µm (**c**) 10% CDW 150-300 µm (**d**) 10% CDW 300-600 µm

texture. This uniformity suggests improved dispersion of hydration products throughout the matrix. The reduction in large, visible voids is likely attributed to CDW's pozzolanic activity, which promotes the formation of C–S–H and refines the pore structure.

Figure 14 presents SEM images captured using secondary electron imaging, showcasing the surface morphologies of various hydration products in specimens containing CDW and TRW. The analysed samples include grouts with 3% TRW, as shown in Fig. 14 a and b. The lower specific gravity of TRW, combined with its tendency to trap air,

led to the formation of voids, as evident in Fig. 14 a. Additionally, air bubbles introduced into the matrix, visible in Fig. 14 b, were observed alongside the hydration products.

In contrast, Fig. 14 c and d depict specimens incorporating CDW, which revealed the presence of C–S–H, C–H, and visible pores. The primary hydration products, C–S–H and C–H, were identified based on their distinct morphologies: C–S–H exhibited a foil-like structure, while C–H appeared as hexagonal, blocky crystals. The pores, visible as dark regions in the SEM images of the hardened grout, suggest incomplete pore refinement. Despite the intention of pozzolanic materials to fill voids and enhance pore structure, the persistence of pores within the grout matrix highlights the limited effectiveness of pore refinement in this case.

Detailed SEM observations revealed clear distinctions in the quality of the interfacial transition zone (ITZ) among the three waste-modified grouts. In the WG series, the ITZ appeared dense and well-integrated, with limited pore continuity and the presence of secondary calcium–silicate–hydrate (C–S–H) phases bridging the glass–matrix interface. These features indicate that the high silica content of finely ground WG particles promoted localized pozzolanic activity and filler effects, resulting in microstructural densification and reduced microcrack density near the interface. In contrast, TRW mixes exhibited discontinuous bonding regions marked by interfacial voids, gaps, and isolated microcracks. The weak ITZ in these samples can be attributed to the hydrophobic surface of the rubber particles and their high deformability, which restrict proper adhesion and cement hydration [61, 66]. For CDW mixes, the ITZ displayed moderate bonding with partial densification, reflecting the heterogeneous nature of the recycled fines. Some regions contained remnant unhydrated cement grains or microvoids surrounded by reaction rims, indicating limited pozzolanic reactivity and weaker interfacial continuity compared to WG.

Although compositional profiling (e.g., EDS line scans) was not performed, the observed microstructural patterns strongly support the mechanical results, namely, the improved stiffness and strength of WG mixes and the reduced load transfer efficiency in TRW-modified grouts. These findings align with previous studies reporting similar ITZ characteristics in cementitious composites containing recycled glass and rubber inclusions [42, 46].

Building upon these ITZ observations, a comparative interpretation of the microstructure–mechanical relationships further substantiates the proposed mechanisms. While detailed quantitative regression between image-derived parameters and mechanical data was beyond the present scope, the qualitative and semi-quantitative analyses indicate clear structure–property correlations across the three waste-modified grout systems. SEM images revealed that WG mixes contained a markedly denser matrix with reduced visible pore area (< 5%), whereas TRW mixes displayed discontinuous interfaces and localised microvoids approaching 10–12% of the image area. CDW mixes exhibited intermediate features, characterised by partially filled pores and heterogeneous particle–matrix contacts. These morphological trends correspond closely with the mechanical outcomes: WG mixes achieved the highest UCS and elastic modulus, TRW mixes the lowest, and CDW mixes moderate values. The observed alignment between matrix compactness and mechanical performance confirms that densification and improved ITZ bonding govern the stiffness–strength response of WG grouts. Future studies will

incorporate quantitative image-based porosity analysis and X-ray micro-computed tomography to further validate these correlations.

4.5 Elemental and phase composition (XRF/XFM analysis)

Elemental analyses of several cementitious grout specimens were performed using the iXRF ATLAS X XRF/XFM system to investigate the influence of WG content and particle size on the grout's chemical composition and phase evolution. As shown in Fig. 15, the elemental maps (Red = Ca, Green = K, Blue = Si) and Ca-normalised compositions collectively indicate that all samples are Ca-dominated matrices characteristic of hydrated cementitious systems, primarily consisting of portlandite and calcium–silicate–hydrate (C–S–H) phases. The incorporation of WG systematically increases the relative Si content, confirming progressive pozzolanic consumption of $Ca(OH)_2$ and formation of more silica-rich C–S–H gels. Finer GP particles (< 75 µm; e.g., samples a and b) produced higher Si/Ca ratios (~ 0.32–0.35) and elevated K/Ca (~ 0.058–0.075), reflecting rapid dissolution and alkali release that enhanced early pozzolanic reactivity and homogeneity of the hydration products. Medium-sized WG (150–300 µm; samples c and d) yielded moderate Si enrichment (Si/Ca ≈ 0.33–0.36) but with visible heterogeneity in the XFM maps, indicating slower reaction kinetics and partially reacted glass grains. Coarse WG (300–425 µm; sample e) exhibited limited surface reaction, as evidenced by patchy Si distribution and localized blue speckles corresponding to unreacted or rim-reacted glass. Higher WG dosages (10–20%), particularly in samples f and g, resulted in pronounced silica enrichment (Si/Ca up to 0.43–0.44) and the most advanced Ca–Si rebalancing, confirming strong pozzolanic activity and refined C–S–H gel formation. Conversely, the control group (sample h, no WG) retained the lowest Si/Ca ratio (~ 0.30), characteristic of a Ca-rich, portlandite-dominated matrix. Across all specimens, Mg, Al, and Fe remained relatively constant (≈ 0.10–0.14, 0.11–0.13, and ≈ 0.05, respectively), demonstrating that the dominant compositional change was the increase in silica and alkali incorporation rather than alterations in secondary oxides. Overall, the results demonstrate that WG content governs the extent of silica enrichment, while particle fineness controls reaction uniformity and kinetics, both contributing to a more refined and chemically stable microstructure in the modified grouts.

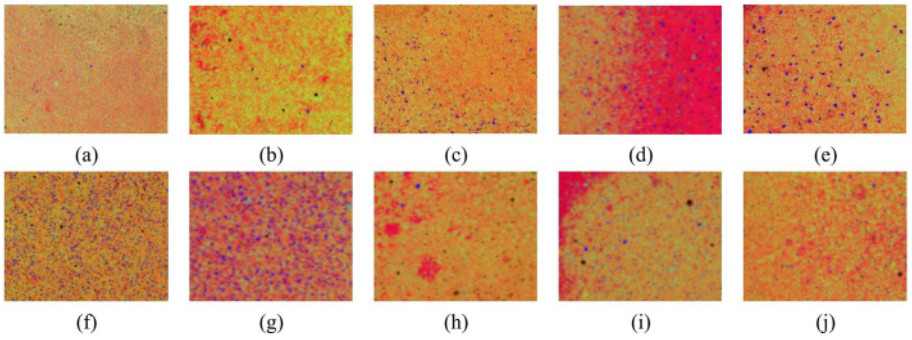

Fig. 15 Elemental XRF/XFM maps of grout specimens incorporating waste glass (WG) at different particle sizes and dosages: (**a**) 10 % WG < 75 µm; (**b**) 2.5 % WG < 75 µm; (**c**) 10 % WG 150–300 µm; (**d**) 5 % WG 150–300 µm; (**e**) 5 % WG 300–425 µm; (**f**) 20 % WG 75-150 µm; (**g**) 20 % WG 150–300 µm; (**h**) control grout (0 % WG) (**i**) 5 % WG 75-150 µm and (**j**) 2.5% WG 75-150 µm. Colour coding: Red = Ca, Green = K, Blue = Si

4.6 Rheological investigation

The shear rate dependence of cementitious grout incorporating glass particles is illustrated in Fig. 16. This behaviour is particularly important for evaluating and controlling the impact of incorporating waste materials on the flowability of grouts, which is a critical property for practical field applications. All mixtures amended by WG exhibited pseudoplastic behaviour, characterised by a decrease in the apparent viscosity with increasing shear rate. This suggests that the internal structure of the grout undergoes a change under shear, leading to reduced resistance to flow.

Focusing on the effect of waste glass, Fig. 16 demonstrates that adding WG consistently reduced the apparent viscosity of the grout across the shear range compared to the control. At equivalent shear rates, WG-modified mixes have lower viscosity, meaning they flow more easily. Mechanistically, several factors contribute to this viscosity drop. First, glass particles have a smooth, non-porous surface and low water absorption, unlike cement grains; thus, they do not demand as much water to wet their surface, nor do they create as much friction between particles. This leads to a more lubricated particle network in the fresh mix. Second, the inclusion of rigid glass disrupts the packing of cement and fly ash particles, creating a less densely crowded particle skeleton within the grout. The resulting internal structure offers less resistance to flow. Furthermore, particle size plays a role: larger WG particles cause a more pronounced decrease in viscosity than finer ones, as observed in the steeper viscosity reduction for mixes with coarser glass. Larger particles present a smaller total surface area to be coated by the cement paste and break up the continuity of the cement matrix, yielding a more fluid, open structure. Overall, the WG-bearing grouts maintained pseudoplasticity while showing significantly lower viscosity at a given shear rate, a favorable outcome for ease of placement.

The TRW-modified grouts displayed a similar shear-thinning profile (Fig. 17), but the magnitude of apparent viscosity change depended on the rubber content and size. At low TRW replacement levels (0.75–1.5% by weight), the viscosity–shear rate curves nearly overlap with that of the plain grout, indicating negligible impact on the mix's flow resistance. However, at the maximum rubber dosage tested (3%), a slight reduction in the apparent viscosity became evident. This reduction was more pronounced when larger rubber particles (300–600 μm) were used. The trend implies that at higher concentrations, and particularly with larger particle sizes, TRW begins to act as a filler that

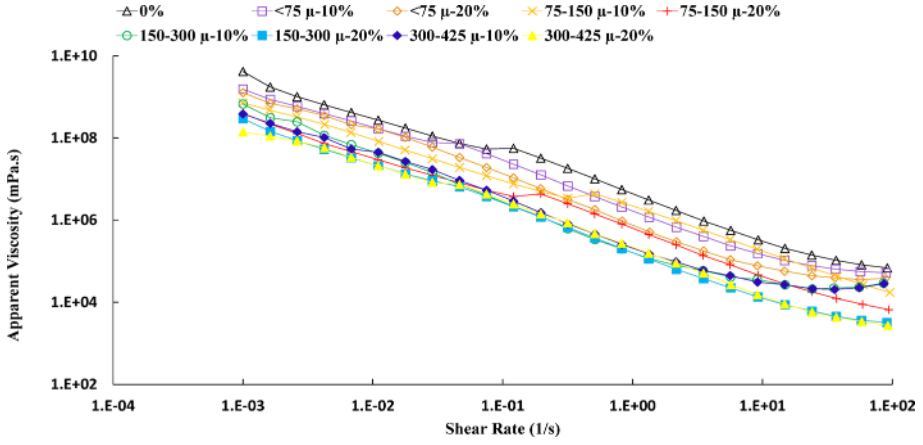

Fig. 16 Viscosity-Shear Rate Behaviour of Cementitious Grouts Incorporating WG

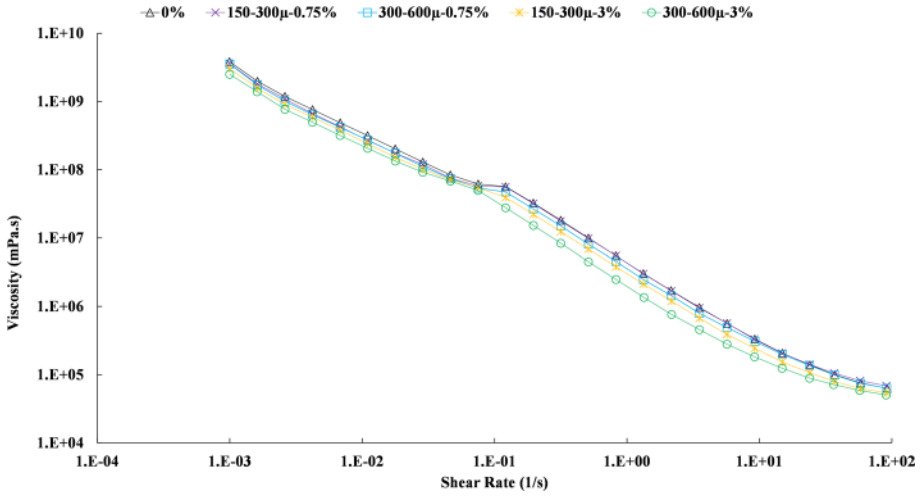

Fig. 17 Rheological behaviour of the cementitious grout incorporating TRW

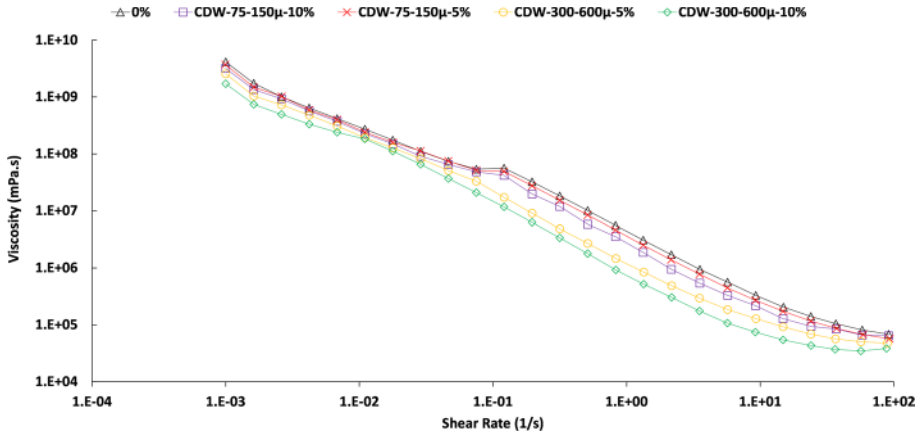

Fig. 18 Rheological behaviour of the cementitious grout incorporating CDW

dilutes and disrupts the cement particle framework, thereby lowering internal friction and yield stress.

The rheological behaviour of cementitious grouts incorporating CDW particles is illustrated in Fig. 18. All mixtures exhibited shear-thinning behaviour, characterised by a decrease in viscosity with increasing shear rate like the other mixtures. Grouts containing 5% CDW with a particle size of 75–150 µm exhibited a negligible decrease in viscosity, while increasing the CDW content to 10% resulted in a slightly more pronounced reduction. A more significant reduction in viscosity was observed for grouts containing 5% and 10% CDW with a particle size of 300–600 µm. These findings suggest that the interaction between CDW particles and the cementitious matrix is influenced by both the CDW content and particle size, with larger particles and higher concentrations leading to more significant reductions in viscosity. This reduction can be attributed to the lower surface area-to-volume ratio of larger particles, which decreases the demand for cement paste to coat the aggregates. Additionally, the higher water absorption capacity of CDW alters the water-to-cement ratio, further influencing the viscosity of the mixture [37, 39].

Although a formal particle-packing model was not employed in this study, the morphology and apparent size distributions of the recycled waste materials were examined using SEM imaging, as shown in Fig. 2. The embedded particle-size annotations on the micrographs indicate that WG and TRW had similar median dimensions, yet their surface textures differed considerably. WG particles exhibited smoother and more compact surfaces, promoting closer packing and reduced inter-particle friction, while TRW particles showed rough, irregular, and porous textures that hindered efficient packing and entrapped air during mixing. CDW particles were coarser and angular, resulting in higher internal friction and water demand.

These morphological attributes correlate directly with the rheological measurements: WG-modified grouts demonstrated the lowest apparent viscosity, followed by CDW and TRW. The improved flowability of WG mixes can thus be attributed to enhanced physical packing and surface smoothness rather than to size refinement alone. Similar behaviour has been reported in earlier studies linking particle morphology to rheological performance in glass-powder and rubber-modified cementitious systems [42, 61, 67]. Future work will incorporate quantitative particle-packing models to validate these qualitative correlations and establish predictive relationships between morphology, packing efficiency, and grout rheology.

4.7 Flow table measurements

The flow table results for cementitious grouts incorporating WG, CDW, and TRW particles show a complex relationship between waste material type, content, and particle size on the flowability of the grouts. As illustrated in Fig. 19 , while a consistent trend was not observed for all mixtures, several general observations can be made. Increasing the content of glass particles generally led to a decrease in flow table diameter, indicating reduced flowability. However, the effect of particle size on flowability was less consistent, with some mixtures showing a decrease in flowability with increasing particle size while others showed no significant change or even an increase. CDW particles had a less pronounced effect on flowability compared to glass particles, with most mixtures exhibiting a slight increase or no change in flow table diameter. TRW particles also had a limited impact on flowability, with most mixtures showing slight increases in flow table diameter. Overall, the results suggest that the interaction between waste material particles and the cementitious matrix is complex and influenced by various factors, including particle type, size, and content.

While the rheological studies consistently showed a decrease in viscosity with increasing shear rate, indicating pseudoplastic behaviour, the flow table results were less consistent. This inconsistency observed between the rheometer and flow table test results is attributable to the fundamentally different stress conditions and measurement principles underlying the two methods. The rotational rheometer evaluates grout behaviour under controlled, continuous shear, allowing for precise quantification of yield stress, plastic viscosity, and shear-thinning behaviour across a defined shear rate range. In contrast, the flow table test simulates a static, low-stress field condition in which the grout's ability to deform and spread is governed primarily by its static yield stress and early structural rigidity. This means that highly thixotropic or shear-sensitive materials, such as the WG-modified grouts, may not fully exhibit their flow potential in the flow table test due to insufficient shear activation. Furthermore, the test's sensitivity to initial paste

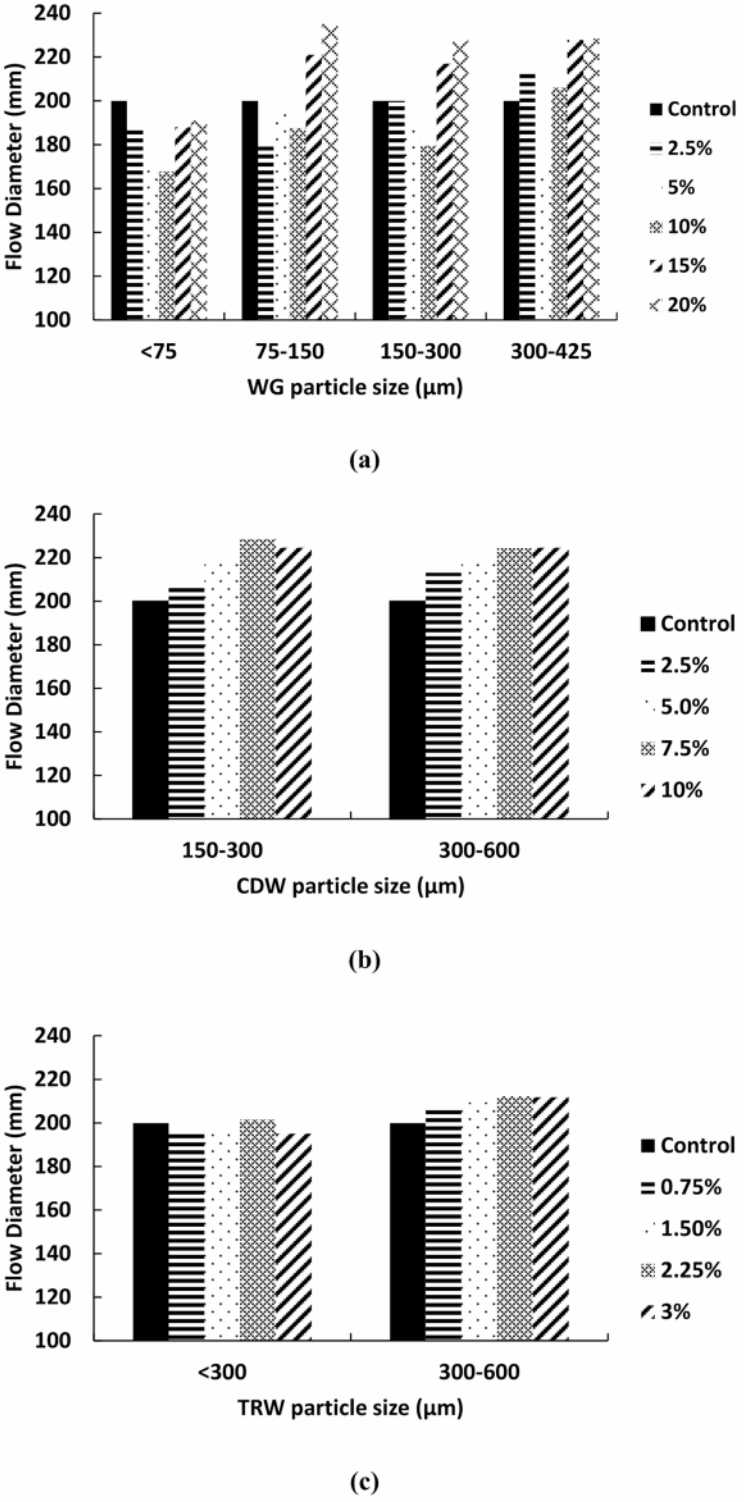

Fig. 19 Flow table results for cementitious grouts incorporating recycled waste materials

structuring, surface friction, and gravitational drainage introduces variability not present in rheometer-based measurements.

From a field perspective, this discrepancy underscores the limitations of the flow table test in predicting actual pumpability and flow performance, particularly for advanced

grout systems exhibiting pseudoplastic behaviour. While the flow table remains a useful screening tool for assessing general workability under gravity-fed conditions (e.g., grouting via chutes or formworks), it does not replicate the pressure-driven, shear-dependent conditions encountered during pump injection of grouts into boreholes for rock reinforcement. As such, rheometer data should be considered more representative of in-situ grout flow behaviour, especially for fully grouted rock bolts or cable bolts where optimal flow under confinement is critical. The practical implication is that grout formulations showing moderate flow table spread may still exhibit excellent pumpability and encapsulation in the field, provided their rheological profiles demonstrate favourable shear-thinning and viscosity control under dynamic loading.

4.8 Improvement of UCS by adjusting water content considering rheological behaviour

Based on the experimental investigation, it was observed that lower water content in grout mixtures enhances the UCS of the samples. Therefore, it was hypothesised that the reduction in UCS caused by incorporating waste materials could be offset by reducing the water content in these mixtures, as the viscosity decreases in samples containing waste materials compared to plain grout. To address this, further experiments were conducted to determine the optimal water content while maintaining identical rheological characteristics in samples containing WG. The results revealed that the viscosity of samples incorporating 5% WG with a water content of 35%–37.5% matched that of plain grout with a water content of 40%. Consequently, 24 additional mixes were prepared, incorporating 5% WG with varying particle sizes (< 75 µm, 75–150 µm, 150–300 µm, and 300–425 µm) and two water contents, 35% and 37.5%. The UCS results, as shown in Fig. 20 , indicate that this adjustment in water content led to an enhancement in strength across various particle sizes of WG. As shown, the reference grout with a water-to-glass (W/G) ratio of 40% achieved a UCS of 67.2 MPa. In comparison, grout with 5% glass particles below 75 µm and a reduced W/G ratio of 35% achieved a 7.7% improvement in UCS. Similarly, grout containing WG particles between 75 and 150 µm demonstrated a 10.6% increase in UCS when the water content was reduced. This innovative modification optimises the balance between rheological behaviour and mechanical performance, offering a sustainable improvement in grout design.

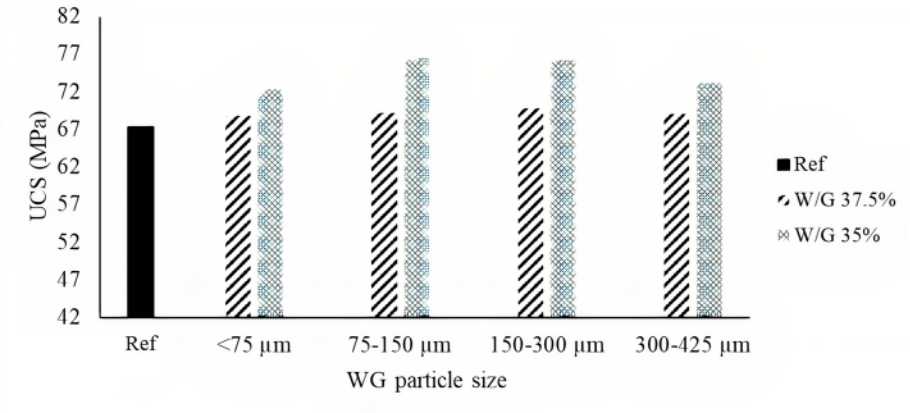

Fig. 20 UCS of Grout Samples containing 5% WG with varying particle sizes and water content of 35% and 37.5%. The water content of the reference mix was 40%

Table 3 Mechanistic influences of recycled waste materials in cementitious Grout formulations

Material	Dominant mechanism	Effect on microstructure	Impact on rheology	Influence on strength and stiffness
Waste Glass (WG)	Pozzolanic reaction (amorphous silica reacts with $Ca(OH)_2$) and micro-filler effect.	Dense C–S–H matrix; refined pores; fewer cracks due to secondary hydration.	Improves flowability; reduces yield stress and plastic viscosity.	Preserves or enhances UCS and E at low content; declines at high content.
Tyre Rubber Waste (TRW)	Inert, elastic inclusion; hydrophobic nature introduces air voids and poor matrix bonding.	Porous, weak interface zones; air voids and heterogeneity increase.	Reduces workability; increases viscosity; entrains air.	Significant UCS and E reduction; improves ductility but lowers rigidity.
Construction & Demolition Waste (CDW)	Physical filler action with limited pozzolanic activity; acts mainly as micro-aggregate.	Moderate pore filling; low hydration contribution; heterogeneous matrix.	Slightly decreases slump; higher water demand due to angular particles.	Moderate strength reduction at low content; more at high content due to dilution.

To consolidate the observed mechanical, rheological, and microstructural behaviour across different grout formulations, a comparative summary of the underlying mechanisms for each recycled waste material is presented in Table 3. This table outlines the dominant chemical or physical mechanisms, their impact on microstructure and rheology, and their net influence on strength and stiffness. The summary highlights how each material uniquely interacts with the cementitious matrix and guides performance-based mix optimisation strategies.

4.9 Practical implications for engineering application

The findings of this study offer important insights into the practical implementation of sustainable grout formulations in underground mining and civil tunnelling projects. By systematically evaluating the mechanical, rheological, and microstructural responses of grout systems modified with waste glass (WG), tyre rubber waste (TRW), and construction and demolition waste (CDW), the results enable targeted decision-making for engineering applications where both performance and environmental accountability are required.

The use of finely ground waste glass (particularly at 2.5% dosage with <75 μm particles) was found to maintain compressive strength and stiffness at levels statistically equivalent to conventional cementitious grout. Moreover, the enhanced flowability and reduced viscosity of WG-modified mixes improve pumpability and encapsulation—two critical factors for achieving complete borehole filling and reliable load transfer in fully grouted rock bolts or cable bolts. Importantly, these benefits are achieved without the need for chemical admixtures, making WG a drop-in replacement that aligns well with current injection and mixing practices in the field [41]. While TRW and CDW may also reduce viscosity, their negative impacts on compressive strength and microstructural cohesion suggest they are less suitable for applications requiring high bond integrity or long-term load bearing [61].

From a cost perspective, replacing even a modest proportion of cement with industrial waste materials presents tangible economic and environmental advantages. Cement is both energy-intensive and expensive to produce; partial substitution with recycled fines can reduce material costs by an estimated 5–10% depending on local waste processing availability [33]. Waste glass, in particular, is widely accessible from municipal recycling streams and requires only mechanical grinding, making it a cost-competitive

additive. Additionally, reduced water demand due to improved flow properties allows for lower water-to-binder ratios, further enhancing mechanical performance while reducing shrinkage-related defects. The elimination of chemical flow enhancers or silica fume, often used to improve pumpability, also contributes to lifecycle cost savings [60].

Field applicability hinges not only on early-age performance but also on durability and bond retention over time. The denser, C–S–H-rich microstructure observed in WG-based mixes is expected to improve resistance to water ingress, sulfate attack, and microcracking—key degradation mechanisms in underground environments. Enhanced packing and secondary hydration effects from pozzolanic reactions suggest that WG incorporation may extend the service life of grouted bolts in aggressive mining conditions [63]. Although long-term field trials are required to quantify these effects under real loading and groundwater exposure, the lab-scale durability indicators support WG's suitability for full-scale deployment. In contrast, TRW and CDW mixes showed microstructural discontinuities and entrained voids, which may accelerate degradation in moist or chemically aggressive strata [21]. As such, their use may be better confined to non-critical reinforcement or temporary support applications where long-term load transfer is not essential.

4.10 Summary of discussions

Overall, the experimental program demonstrated that incorporating WG, TRW, and CDW into cementitious grout can meaningfully influence both mechanical and rheological performance. WG emerged as the most promising additive, preserving or even enhancing compressive strength and stiffness at low dosages, particularly when particle sizes were below 75 μm. This behaviour is consistent with previous work showing that fine waste glass can densify the matrix and improve pumpability through pozzolanic and filler effects [45, 49]. By contrast, TRW and CDW caused more pronounced strength reductions due to hydrophobicity, porosity, and binder dilution, although both contributed positively to ductility and rheological behaviour.

The strengths of this study lie in its comprehensive experimental design, encompassing 740 UCS samples, microstructural imaging, rheological testing, and flow-table assessments. This systematic approach enables reliable comparisons across waste types and replacement levels. Importantly, coupling rheological optimisation with mechanical evaluation provided a methodological advance, as most earlier studies considered these aspects separately [47, 48]. The demonstration that targeted water-content adjustments can recover or even surpass baseline strength highlights the potential of performance-based optimisation for sustainable grout design.

Limitations must also be noted. Durability and field pull-out testing were not undertaken, though they are essential for confirming long-term bond performance under real conditions. While SEM observations indicated improved pore refinement in WG mixes, durability should be verified through field or accelerated testing. Additionally, the performance of TRW and CDW was more variable and particle-size sensitive, suggesting that further optimisation or surface treatment may be required for consistent results.

Implications for methodology are significant. The results support integrating microstructural and rheological profiling with mechanical testing as a standardised framework for evaluating sustainable grouts. Such integration goes beyond traditional UCS benchmarks, ensuring that environmentally motivated substitutions also meet practical

requirements for pumpability, encapsulation, and load transfer. This direction aligns with recent methodological frameworks proposed for sustainable aggregates and cementitious systems [49, 56]. By positioning recycled-waste grout design within this broader methodological context, the present study advances both the scientific and applied understanding of sustainable ground reinforcement.

4.11 Design code limitations and requirements

An essential consideration for the implementation of sustainable grout formulations is compliance with established design codes and specifications. Current international and domestic standards, such as ASTM C109/C109M-24 [9] for compressive strength, ASTM C230/C230M-23 [12] for flow behaviour, and the Australian Standards AS 1012.9 [4] and AS 2701-2001 (R2015) [7], provide well-defined procedures for evaluating the mechanical and rheological performance of grouts. However, these codes focus largely on traditional Portland cement-based systems and do not provide explicit provisions for the inclusion of recycled waste materials such as finely ground glass, tyre rubber, or construction and demolition fines.

In structural design codes, including Eurocode 2 EN 1992-1-1 [28] and the Australian Concrete Structures Code [8], the use of supplementary cementitious materials (SCMs) like fly ash, slag, and silica fume is recognised and regulated. By contrast, recycled waste streams such as waste glass and CDW are not formally codified, meaning their application must be justified through performance testing rather than prescriptive allowances. Rubber inclusions face even greater constraints, as most codes note reductions in elastic modulus and bond performance that limit their use in structural or load-bearing grouts without additional qualification testing.

Recent international research has highlighted this gap and called for the systematic inclusion of recycled aggregates in standards, with attention to durability, shrinkage, and long-term bond integrity [34, 44, 45]. These studies reinforce the need to update codes to explicitly address non-traditional waste materials and provide performance-based acceptance criteria.

The findings of this study align with code-based performance thresholds in terms of compressive strength and flowability. For example, grouts incorporating 5% finely ground WG (<75 μm) achieved compressive strength values statistically comparable to control mixes, thereby satisfying typical structural strength requirements in AS 3600 [8]. Furthermore, the observed rheological improvements at low WG contents support field pumpability demands outlined in practical grouting guidelines. Nonetheless, broader adoption of TRW and CDW in codified practice requires further validation, particularly regarding durability and long-term bond performance, before they can be formally integrated into design codes. Overall, while recycled waste materials demonstrate strong potential for sustainable grout formulations, their uptake in engineering practice will remain limited until standards evolve to explicitly permit and regulate their use. This underscores the importance of performance-based testing frameworks and the continued development of code provisions that reflect advances in sustainable construction materials.

5 Conclusions

This research investigated the feasibility of incorporating recycled waste materials (waste glass (WG), tyre rubber waste (TRW), and construction demolition waste (CDW)) into cementitious grout for cable bolting applications. To evaluate the impact of these waste materials on the grout's properties, a comprehensive experimental program was conducted. The study focused on assessing compressive strength, elastic modulus, macro-micro structural analysis, and rheological properties.

The compressive strength and elastic modulus of grout samples incorporating WG powder (2.5–20%), TRW (0.75–3%), and CDW (2.5–10%) by weight were investigated across various particle size ranges. The incorporation of waste materials resulted in distinct performance trends. Among all tested mixtures, those incorporating 2.5% WG with < 75 μm particles achieved compressive strength values up to 97% of the control (70.5 MPa), maintaining structural integrity without significant compromise. In contrast, TRW- and CDW-modified mixes showed UCS reductions of 21.6% and 19.9%, respectively, at their optimal dosages (0.75% TRW < 300 μm and 2.5% CDW 150–300 μm), indicating more pronounced trade-offs between sustainability and strength. When water content was adjusted to match target rheology, 5% WG mixes yielded up to 10.6% higher UCS than the control grout, demonstrating that mechanical performance can be recovered or even improved through careful balance of rheological and compositional parameters. These findings not only affirm the potential of WG as a cement substitute but also underscore the critical role of particle size, replacement dosage, and water optimisation in maximising the structural benefits of sustainable grout formulations.

Macro analysis revealed a uniform distribution of WG particles with minimal segregation but noted the formation of pores that could compromise strength. SEM analysis confirmed that partial replacement with WG powder enhances grout structure through pozzolanic reactions and the filler effect, although higher replacement levels reduce binder production and compactness. Macro-scale and SEM images of grouts incorporating CDW and TRW showed that CDW promotes a more uniform and denser matrix, while TRW introduces air voids due to its lower specific gravity. Despite some limitations, these materials demonstrate promise in enhancing grout performance, particularly in optimizing strength and homogeneity at appropriate replacement levels. Rheological testing demonstrated that incorporating waste materials generally decreased apparent viscosity, with the effect intensifying at higher replacement levels and finer particle sizes. The largest viscosity reductions were recorded for 20% WG (300–425 μm), 3% TRW (300–600 μm), and 10% CDW (300–600 μm). Flow-table results were less consistent because this static test cannot fully capture the time-dependent, shear-sensitive behaviour of these thixotropic grouts. The discrepancy between rheometer and flow-table outcomes arises from their differing mechanisms: rheometers apply controlled shear to quantify viscosity and shear-thinning behaviour, whereas flow-tables measure free spread under gravity. Consequently, the rheometer data provide a more realistic indication of pumpability and field performance for waste-modified grouts.

To bridge the gap between laboratory performance and field applicability, it is recommended that future investigations explore the pull-out capacity of cable bolts grouted with the top-performing mix designs identified in this study. While this research focused on mechanical and rheological characterisation to screen the suitability of various recycled material combinations, the ultimate validation of optimal grout performance lies

in its load transfer efficiency under realistic anchorage conditions. Incorporating pull-out testing in follow-up studies will not only refine the optimal mix proportion but also enable practical engineering adoption, particularly for ground reinforcement in mining and civil tunnelling applications. This integrated approach offers a novel pathway to ensure that sustainability-driven grout formulations also meet structural anchorage demands in real-world settings.

Acknowledgements
The authors would like to acknowledge the in-kind support of Jennmar Australia, Zilch waste recyclers, Tyrecycle and iQRenew.

Author contributions
Conceptualization, A.E., H.N., P.B., K.M., P.C., B.J.S., S.E., N.A., and A.M.; methodology, A.E., H.N., P.B., K.M., P.C., B.J.S., S.E., and A.M.; software, A.E., B.J.S., and S.E.; validation, A.E., H.N., P.B., P.C., B.J.S., S.E. and A.M.; formal analysis, A.E., H.N., P.B., K.M., P.C., B.J.S., S.E., N.A., and A.M.; investigation, A.E., H.N., P.B., K.M., P.C., B.J.S., S.E., N.A., and A.M.; resources, A.E., H.N., P.B., K.M., P.C., B.J.S., S.E., and A.M.; datacuration, A.E., H.N., P.B., K.M., P.C., B.J.S., S.E., N.A., and A.M.; writing—original draft preparation, A.E., H.N., P.B., K.M., and A.M.; writing—review and editing, A.E., H.N., P.B., K.M., P.C., B.J.S., S.E., N.A., and A.M.; visualization, A.E., H.N., P.B., K.M., P.C., B.J.S., S.E., N.A., and A.M. All authors have read and agreed to the published version of the manuscript.

Funding
This research has been funded by the Australian Department of Education through a Regional Research Collaboration (RRC) grant. This funding has allowed the establishment of the University of Southern Queensland-led SIMPLE Hub where this research has been conducted.

Data availability
The data supporting the findings of this study are available upon request from the corresponding author.

Declarations

Ethics approval and consent to participate
not applicable.

Consent for publication
not applicable.

Competing interests
The authors declare no competing interests.

Received: 22 August 2025 / Accepted: 11 November 2025
Published online: 29 November 2025

References

1. Adesina A, de Azevedo ARG, Amin M, Hadzima-Nyarko M, Agwa IS, Zeyad AM, Tayeh BA. Fresh and mechanical properties overview of alkali-activated materials made with glass powder as precursor. Cleaner Mater. 2022. https://doi.org/10.1016/j.clema.2021.100036.
2. Ahmed A. Chemical reactions in pozzolanic concrete. Mod Approaches Mater Sci. 2019. https://doi.org/10.32474/mams.2019.01.000120.
3. Alehossein H, Shen B, Qin Z, Huddlestone-Holmes C. Flow Analysis, transportation, and deposition of frictional viscoplastic slurries and pastes in civil and mining engineering. 2012. https://doi.org/10.1061/(ASCE)MT.1943-5533.
4. AS 1012.9. Methods of testing concrete – Compressive strength tests. Australian Standards; 2014.
5. AS 1141.11.1:2020 Amd 1. Methods for sampling and testing aggregates, Method 11.1: Particle size distribution - Sieving method. Standards Australia; 2022.
6. AS 2350.2. Methods of testing Portland, blended and masonry cements, Method 2: Chemical composition. Standards Australia; 2006.
7. AS 2701–2001 (R2015). Methods of sampling and testing mortar for masonry constructions. Standards Australia; 2015.
8. AS 3600. Concrete structures. Standards Australia; 2018.
9. ASTM C109/C109M-24. Test method for compressive strength of hydraulic cement mortars (Using 2-in. Or [50-mm] cube Specimens). ASTM Int. 2024. https://doi.org/10.1520/C0109_C0109M-20.
10. ASTM C114-24. Standard test methods for chemical analysis of hydraulic cement. ASTM International; 2024.
11. ASTM C136/C136M-19. Standard test method for sieve analysis of fine and coarse aggregates. ASTM International; 2019.
12. ASTM C230/C230M-23. Standard specification for flow table for use in tests of hydraulic cement. ASTM International; 2023.
13. ASTM C305-20. Practice for mechanical mixing of hydraulic cement pastes and mortars of plastic consistency. ASTM Int. 2020. https://doi.org/10.1520/C0305-20.
14. ASTM C1723-25. Standard guide for examination of hardened concrete using scanning electron microscopy. ASTM International; 2025.
15. ASTM C1749-25. Standard guide for measurement of the rheological properties of hydraulic cementitious paste using a rotational rheometer. ASTM International; 2025.

16. Aziminezhad M, Mahdikhani M, Memarpour MM. RSM-based modeling and optimization of self-consolidating mortar to predict acceptable ranges of rheological properties. Constr Build Mater. 2018;189:1200–13. https://doi.org/10.1016/j.conbuildmat.2018.09.019.
17. Aziz N, Nemcik J, Mirzaghorbanali A, Foldi S, Joyce D, Moslemi A, Ghojavand H, Ma S, Li X, Rasekh H. Suggested methods for the preparation and testing of various properties of resins and grouts. In Coal Operators Conference; 2014. (pp. 163–176). https://ro
18. Baikerikar A, Mudalgi S, Ram VV. Utilization of waste glass powder and waste glass sand in the production of Eco-Friendly concrete. Constr Build Mater. 2023. https://doi.org/10.1016/j.conbuildmat.2023.131078.
19. Benmokranet B, Chennouft A, Mitri$ HS. Laboratory evaluation of cement-based grouts and grouted rock anchors. Int J Rock Mech Min Sci & Geomech Abstr. 1995;32(7).
20. Berndt ML. Properties of sustainable concrete containing fly ash, slag and recycled concrete aggregate. Constr Build Mater. 2009;23(7):2606–13. https://doi.org/10.1016/j.conbuildmat.2009.02.011.
21. Braga M, De Brito J, Veiga R. Incorporation of fine concrete aggregates in mortars. Constr Build Mater. 2012;36:960–8. https://doi.org/10.1016/j.conbuildmat.2012.06.031.
22. Cao C, Ren T, Zhang Y, Zhang L, Wang F. Experimental investigation of the effect of grout with additive in improving ground support. Int J Rock Mech Min Sci. 2016;85:52–9. https://doi.org/10.1016/j.ijrmms.2015.12.010.
23. Chen J, Saydam S, Hagan PC. An analytical model of the load transfer behavior of fully grouted cable bolts. Constr Build Mater. 2015;101:1006–15. https://doi.org/10.1016/j.conbuildmat.2015.10.099.
24. de Lima DO, de Lira DS, Rojas MF, Junior HS. Assessment of the potential use of construction and demolition waste (CDW) fines as eco-pozzolan in binary and ternary cements. Constr Build Mater. 2024. https://doi.org/10.1016/j.conbuildmat.2023.134320.
25. Entezam A, Nourizadeh H, Mirzaghorbanali A, Burey P, Mcdougall K, Shokri BJ, Entezam S, Craig P, Aziz N. Sustainability in underground mining and geotechnical practices. 2025 The Resource Operators Conference. 2025.
26. Entezam A, Nourizadeh H, Mirzaghorbanali A, Burey P, Shelley T. Application of waste glass powder in cemenitious grouts. 2024. https://ro
27. Entezam S, Shokri BJ, Nourizadeh H, Motallebiyan A, Mirzaghorbanali A, Aziz N, McDougall K, Karunasena K. Investigation of the effect of using fly ash in the grout mixture on performing the fully grouted rock bolt systems. In Resource Operators Conference; 2023. (pp. 296–301).
28. Eurocode 2 EN 1992-1-1. Design of concrete structures general rules and rules for buildings. European Standards; 2015.
29. Getachew EM, Yifru BW, Taffese WZ, Yehualaw MD. Enhancing mortar properties through thermoactivated recycled concrete cement. Buildings. 2023. https://doi.org/10.3390/buildings13092209.
30. Hajimohammadi A, Ngo T, Kashani A. Glass waste versus sand as aggregates: the characteristics of the evolving geopolymer binders. J Clean Prod. 2018;193:593–603. https://doi.org/10.1016/j.jclepro.2018.05.086.
31. Hosseini S, Entezam S, Jodeiri Shokri B, Mirzaghorbanali A, Nourizadeh H, Motallebiyan A, Entezam A, McDougall K, Karunasena W, Aziz N. Predicting grout's uniaxial compressive strength (UCS) for fully grouted rock bolting system by applying ensemble machine learning techniques. Neural Comput Appl. 2024. https://doi.org/10.1007/s00521-024-10128-y.
32. Imbabi MS, Carrigan C, McKenna S. Trends and developments in green cement and concrete technology. Int J Sustain Built Environ. 2012;1(2):194–216. https://doi.org/10.1016/j.ijsbe.2013.05.001.
33. Islam GMS, Rahman MH, Kazi N. Waste glass powder as partial replacement of cement for sustainable concrete practice. Int J Sustain Built Environ. 2017a;6(1):37–44. https://doi.org/10.1016/j.ijsbe.2016.10.005.
34. Jiang Y, Ling TC, Mo KH, Shi C. A critical review of waste glass powder – multiple roles of utilization in cement-based materials and construction products. J Environ Manage. 2019;242:440–9. https://doi.org/10.1016/j.jenvman.2019.04.098.
35. Jodeiri Shokri B, Mirzaghorbanali A, Nourizadeh H, McDougall K, Karunasena W, Aziz N, et al. Axial load transfer mechanism in fully grouted rock bolting system: a systematic review. Appl Sci. 2024. https://doi.org/10.3390/app14125232.
36. Kang H, Li W, Gao F, Yang J. Grouting theories and technologies for the reinforcement of fractured rocks surrounding deep roadways. Deep Underground Sci Eng. 2023;2(1):2–19. https://doi.org/10.1002/dug2.12026.
37. Kim N, Kim J. Effect of maximum aggregate size and powder content on the properties of self-compacting recycled aggregate concrete. Period Polytech Civ Eng. 2023;67(4):1038–47. https://doi.org/10.3311/PPci.20407.
38. Lekkam M, Benmounah A, Kadri EH, Soualhi H, Kaci A. Influence of saturated activated carbon on the rheological and mechanical properties of cementitious materials. Constr Build Mater. 2019;198:411–22. https://doi.org/10.1016/j.conbuildmat.2018.11.257.
39. Lima PRL, Filho RDT, Da Fonseca Martins Gomes O. Influence of recycled aggregate on the rheological behavior of cement mortar. Key Eng Mater. 2014;600:297–307. https://doi.org/10.4028/www.scientific.net/KEM.600.297.
40. Liu J, Li Y, Zhang G, Liu Y. Effects of cementitious grout components on rheological properties. Constr Build Mater. 2019. https://doi.org/10.1016/j.conbuildmat.2019.08.035.
41. Liu M. Incorporating ground glass in self-compacting concrete. Constr Build Mater. 2011;25(2):919–25. https://doi.org/10.1016/j.conbuildmat.2010.06.092.
42. Mejdi M, Wilson W, Saillio M, Chaussadent T, Divet L, Tagnit-Hamou A. Hydration and microstructure of glass powder cement pastes – a multi-technique investigation. Cem Concr Res. 2022. https://doi.org/10.1016/j.cemconres.2021.106610.
43. Mikos AP, Ng CWW, Faro VP. Sustainable application of fine recycled-concrete aggregate in soil-nailing grout. J Mater Civ Eng. 2021. https://doi.org/10.1061/(asce)mt.1943-5533.0003814.
44. Mohanta NR, Murmu M. Alternative coarse aggregate for sustainable and eco-friendly concrete - a review. J Build Eng. 2022. https://doi.org/10.1016/j.jobe.2022.105079.
45. Mohanta NR, Murmu M. Performance assessment of Linz–Donawitz slag as alternative coarse aggregate in concrete: a comprehensive study on mechanical and durability properties. Innov Infrastruct Solut. 2023. https://doi.org/10.1007/s41062-023-01257-9.
46. Mohanta NR, Murmu M. Comparative study on the effect of incorporation of Linz-Donawitz slag as coarse aggregate in concrete reinforced with different fibers. Innov Infrastruct Solut. 2024. https://doi.org/10.1007/s41062-024-01387-8.
47. Mohanta NR, Murmu M. A review on the utilization of steel slag as alternative coarse aggregate in concrete: transforming waste into wealth. In Iranian journal of science and Technology - Transactions of civil engineering. Springer Science and Business Media Deutschland GmbH; 2025. https://doi.org/10.1007/s40996-025-01981-5.

48. Mohanta NR, Murmu M. Evaluating the co-relationship between the mechanical properties of steel slag aggregate concrete reinforced with steel fiber. Eng Res Express. 2025c. https://doi.org/10.1088/2631-8695/ade6cb.
49. Mohanta NR, Murmu M. Exploring the combined impact of coarse linz-donawitz slag and basalt fiber on the properties of concrete. J Build Pathol Rehabil. 2025;10(1): 20. https://doi.org/10.1007/s41024-024-00528-x.
50. Murmu M, Ranjan Mohanta N, Bapure N. Study on the fresh and hardened properties of concrete with steel slag as partial replacement for natural aggregates. Mater Today Proc. https://doi.org/10.1016/j.matpr.2023.03.151.
51. Nassar RUD, Soroushian P. Strength and durability of recycled aggregate concrete containing milled glass as partial replacement for cement. Constr Build Mater. 2012;29:368–77. https://doi.org/10.1016/j.conbuildmat.2011.10.061.
52. Ni JC, et al. Monitoring and modeling grout efficiency of liftingstructure in soft clay. Am Soc Civil Eng. 2010;223–9. https://doi.org/10.1061/(ASCE)GM.1943-5622.0000026.
53. Pickin J, Wardle C, O'farrell K, Stovell L, Nyunt P, Guazzo S, Lin Y, Caggiati-Shortell G, Chakma P, Edwards C, Lindley B, Latimer G, Downes J, Axiö I, Reviewers R. Australian Government & Blue Environment 2022, National Waste Report 2022, Department of Climate Change Energy the Environment and Water, Version Final (1.2); 2022. https://www
54. Rahman M, Wiklund J, Kotzé R, Håkansson U. Yield stress of cement grouts. Tunn Undergr Space Technol. 2017;61:50–60. https://doi.org/10.1016/j.tust.2016.09.009.
55. Ranjan Mohanta N, Murmu M. Evaluating the fresh and mechanical properties of steel slag aggregate concrete reinforced with steel fiber. Mater Today Proc. 2024. https://doi.org/10.1016/j.matpr.2024.04.093.
56. Ranjan Mohanta N, Samantaray S. Study of combined effect of Metakaolin and steel fiber on mechanical properties of concrete. Pertanika J Sci Technol. 2019;27(3):1381–96.
57. Rashid K, Hameed R, Ahmad HA, Razzaq A, Ahmad M, Mahmood A. Analytical framework for value added utilization of glass waste in concrete: mechanical and environmental performance. Waste Manag. 2018;79:312–23. https://doi.org/10.1016/j.wasman.2018.07.052.
58. Rocha JHA, Toledo Filho RD, Cayo-Chileno NG. Sustainable alternatives to CO2 reduction in the cement industry: a short review. Mater Today Proc. 2022;57:436–9. https://doi.org/10.1016/j.matpr.2021.12.565.
59. Shahidan S, Azmi MAM, Kupusamy K, Zuki SSM, Ali N. Utilizing construction and demolition (C&D) waste as recycled aggregates (RA) in concrete. Procedia Eng. 2017;174:1028–35. https://doi.org/10.1016/j.proeng.2017.01.255.
60. Shayan A, Xu A. Performance of glass powder as a pozzolanic material in concrete: a field trial on concrete slabs. Cem Concr Res. 2006;36(3):457–68. https://doi.org/10.1016/j.cemconres.2005.12.012.
61. Siddika A, Mamun M. A. Al, Alyousef R, Amran YHM, Aslani F, Alabduljabbar H. Properties and utilizations of waste tire rubber in concrete: a review. Constr Build Mater. 2019a;224:711–31. https://doi.org/10.1016/j.conbuildmat.2019.07.108.
62. Sui Y, Ou C, Liu S, Zhang J, Tian Q. Study on properties of waste concrete powder by thermal treatment and application in mortar. Appl Sci. 2020. https://doi.org/10.3390/app10030998.
63. Taha B, Nounu G. Utilizing waste recycled glass as sand/cement replacement in concrete. J Mater Civ Eng. 2009;21(12):709–21. https://doi.org/10.1061/(asce)0899-1561(2009)21:12(709).
64. Wu C, Zhou X, Wang L, Li Z, Zhang X. Failure mechanism of full-length grouted bolts for large-deformation tunnels under high geo-stress: a case study. Eng Fail Anal. 2024. https://doi.org/10.1016/j.engfailanal.2024.108021.
65. Xiao J, Li L, Shen L, Poon CS. Compressive behaviour of recycled aggregate concrete under impact loading. Cem Concr Res. 2015;71:46–55. https://doi.org/10.1016/j.cemconres.2015.01.014.
66. Xu J, Houndehou JD, Wang Z, Ma Q. Experimental investigation on the mechanical properties and damage evolution of steel-fiber-reinforced crumb rubber concrete with porcelain tile waste. Constr Build Mater. 2023. https://doi.org/10.1016/j.conbuildmat.2023.130643.
67. Yin W, Li X, Sun T, Chen Y, Xu F, Yan G, et al. Utilization of waste glass powder as partial replacement of cement for the cementitious grouts with superplasticizer and viscosity modifying agent binary mixtures: rheological and mechanical performances. Constr Build Mater. 2021. https://doi.org/10.1016/j.conbuildmat.2021.122953.
68. Yokota Y, Zhao Z, Nie W, Date K, Iwano K, Okada Y. Experimental and numerical study on the interface behaviour between the rock bolt and bond material. Rock Mech Rock Eng. 2019a;52(3):869–79. https://doi.org/10.1007/s00603-018-1629-4.
69. Yuan W, Yang R, Yu J, Zhou S, Cui S, Kang J, Yao Z. Preparation and properties study of cementitious grouts containing crumb rubber. Buildings. 2021. https://doi.org/10.3390/buildings11110555.
70. Zhang C, Cui G, Chen X, Zhou H, Deng L. Effects of bolt profile and grout mixture on shearing behaviors of bolt-grout interface. J Rock Mech Geotech Eng. 2020;12(2):242–55. https://doi.org/10.1016/j.jrmge.2019.10.004.
71. Zhang S, Luan H, Jiang Y, Wang Y, Li B, Liu Z, et al. Study on the load transfer and damage evolution characteristics of the bolt-grout interface concerning bolt rib parameters: based on a finite-discrete numerical method. Comput Geotech. 2025. https://doi.org/10.1016/j.compgeo.2024.107010.

Publisher's note